The HR Diagram and the Galactic distance scale after Hipparcos

I. Neill Reid
Palomar Observatory, 105-24, California Institute of Technology, Pasadena, CA 91125, e-mail: inr@astro.caltech.edu

ABSTRACT

The completion and publication of the Hipparcos astrometric catalogue has revitalised studies in many fundamental areas of Galactic structure and stellar evolution. This article reviews the impact of the new parallax results on our understanding of the location of the main-sequence as a function of abundance, of the luminosity calibration of primary distance indicators and of the Galactic distance scale. Many of these issues remain to be resolved.

Subject headings: Stars: subdwarfs, parallaxes, RR Lyraes; Globular clusters: distances; Galactic structure

1. Introduction

Calibration of the extragalactic distance scale rests on our ability to determine accurate locations in the observational Hertzsprung-Russell diagram for specific types of stars at particular stages in their evolution. Whether one uses Cepheids, RR Lyraes, planetary nebulae or type I supernovae as links in the distance chain, the underlying assumptions are that in matching similar types of stars in different stellar systems, one is comparing like with like; and that if the calibrators are not identical, systemic variations can be traced to systematic trends with changes in physical characteristics. Given that those criteria are satisfied, in principle all distance-scale investigations can determine *relative* distances between different external galaxies. However, determining absolute distances requires absolute luminosities for individual calibrators. Thus, the accuracy with which one can derive parameters such as the Hubble constant, H_0, depends on the accuracy with which one can measure distances within the Galaxy so as to calibrate the various distance indicators.

Trigonometric parallax measurements offer the only method of directly measuring distances to almost all single stars or muliple star systems. The application of CCD detectors to astrometry (Monet, 1988) has shown that sub-milliarcsecond (mas) precision can be achieved from the ground. However, the need for adequate reference stars within the small field of view allowed by current CCDs limits observations to faint apparent magnitudes ($V \geq 14$), and hence to nearby stars of low intrinsic luminosities. Moreover, the accuracy of the final parallax is dependent on the transformation from relative to absolute reference frames.

The ESA Hipparcos satellite was designed to address this issue. Full details of the scope of this mission and the subsequent analysis are given by van Leeuwen (1997) and Kovalevsky (1998). Two 13-cm diameter optical telescopes were used to image 1 square-degree regions of the sky, separated by 58^o, onto the same focal plane. A photodiode timed stellar transits across a reference grid as the satellite rotated on its axis. Ground-based parallax observations are limited to small angular fields of view, and reference stars share the same parallactic motion as the target - hence the necessity for correction from relative to absolute systems. Hipparcos measured angular separations of stars with significantly different parallax factors, allowing direct determination of absolute parallaxes in the final astrometric solution.

Hipparcos was a targeted mission, rather than a sky survey, with programme objects limited generally to surface densities of eight per square degree. Photon-counting statistics rendered impracticable observations of sources fainter than 13th magnitude. The final catalogue includes positions, proper motions and parallax measurements, as well as BV photometry, for 118,000 stars, including nearly every star brighter than 7th visual magnitude, but for only 45,000 stars with $9 < V < 11$ and 4,000 stars between 11th and 13th magnitude.

These data have formed the basis for a large number of investigations over the last two years (160 refereed publications as of May, 1998). The present article does not aim at a comprehensive review of all issues raised in those papers. Rather, our intention is to consider the impact of the

Hipparcos results on investigations of the distance scale. This leads us to focus on two issues: the location of the main-sequence as a function of age and chemical abundance, based partly on observations of nearby stars and partly on distance estimates to clusters; and direct distance measurements of primary distance indicators. We consider how these re-calibrations affect distance estimates to the Magellanic Clouds and M31, but carry extragalactic distance scale arguments no further.

2. Astrometric accuracy and systematic biases

2.1. Measurement precision

The formal precision of the astrometry for an individual star depends primarily on the number of observations and the signal-to-noise of each observation. Scans were made with the satellite rotational axis precessing at 6.4 revolutions yr^{-1} at an angle of 43^o to the direction to the Sun. As a result, stars at ecliptic latitudes $\beta > 47^o$ (particularly those at $\beta \sim 47^o$) were observed more frequently than those at lower latitudes, with a corresponding $\sim 50\%$ increase in accuracy (ESA, 1997). Figure 1 illustrates the typical distribution of formal uncertainties $(\sigma_{\mu(\alpha)}, \sigma_{\mu(\delta)}, \sigma_\pi)$ as a function of apparent magnitude.

Data reduction was undertaken independently by two consortia, NDAC and FAST, with the final catalogue consisting of the merged astrometric parameters. Both undertook extensive tests and comparisons to verify the accuracy of the satellite astrometry, particularly the reliability of the absolute zeropoints in μ and π. Those tests are discussed by Arenou et al (1995), Lindegren et al (1995) and Lindegren (1995) for the initial 30-month analysis, and in the first and third volumes of the Hipparcos catalogue (ESA, 1997). In brief, the positional data show clear evidence for distortions in the FK5 ground-based frame at the 60-100 milliarcsecond level, while a comparison of the proper motions against ground-based data, which have longer time baselines and comparable accuracy, confirms random uncertainties of $\epsilon_H(\mu) \sim 1 - 2$ mas. Similarly, comparisons of the Hipparcos parallax data against the most accurate available ground-based measurements (by the US Naval Observatory) generally confirm the 1-2 mas quoted uncertainties of individual observations, as does Lindegren's (1995) analysis of the distribution of negative parallaxes.

Determining the reliability of the absolute zeropoints, notably in parallax, is a more complex issue. Co-ordinates are on the J2000 system (epoch 1991.25), referenced to the International Celestial Reference System (ICRS) via secondary standards (no extragalactic reference sources were observable by Hipparcos). The zeropoint for the proper-motion system is tied to the extragalactic frame through reference sources with absolute motions, either directly from VLBI or indirectly, from photographic surveys (see Johnson, 1999, this volume). The zeropoint of the Hipparcos parallaxes, π_H, was tested by matching against independent parallax estimators (e.g. photometric parallax), primarily for distant stars where $\sigma_\pi(other) << \sigma_\pi(H)$. In particular, Hipparcos data for 46 Magellanic Cloud stars ($\pi \approx 0.02$ mas) give $\bar{\pi} = -0.16 \pm 0.26$ mas and

$\sigma_\pi = 1.72 \pm 0.18$ mas. Arenou et al conclude that the overall results are consistent with a *global* zeropoint error of < 0.1 mas in π_H. However, this does not exclude larger deviations on smaller angular scales, as discussed further below.

These tests of the parallax zeropoint rest primarily on relatively faint stars, since few stars brighter than 7th magnitude have high-accuracy ground-based parallaxes. Harris et al (1997) and Gatewood et al (1998) present comparisons based on 23 and 63 stars respectively. A weighted mean of their results (Hanson, priv. comm.) gives $\pi_H - \pi_{other} = 0.30 \pm 0.24$mas, where the uncertainty is the standard error of the mean. While this is consistent with the absolute zeropoint defined at fainter magnitudes, they fail to provide a stringent test of the presence of any magnitude-dependent systematics.

2.2. Systematic biases in parallax determination

Lutz-Kelker bias

The measured parallax provides the best (trigonometric) estimate of the distance to a particular star system. If, however, one considers that same object in a statistical sense - as a representative of the disk main sequence, for example - then one must allow for possible systematics introduced by the sample-selection criteria adopted. This potential for bias in statistical analysis of parallax-selected datasets was noted early this century by Russell and is also discussed by Trumpler & Weaver (1953). Lutz & Kelker (1973) provide the first quantitative description of this effect.

Under the standard assumption that the measured parallax, π_o, is an unbiased estimate of the true parallax, π, the conditional distribution $C_o(\pi_o|\pi)$ has a mean value π. However, we are aiming to determine π given π_o, and are therefore concerned with the conditional distribution $C(\pi|\pi_o)$. In that case,

$$C(\pi|\pi_o) \quad \sim \quad C_o(\pi_o|\pi) * N_D(\pi) \tag{1}$$

where $N_D(\pi)$ is the true parallax distribution of stars in dataset D. Note that $N_D(\pi)$ is often *not* identical with the parallax distribution of the parent Galactic stellar population, since D is usually pre-selected based on a combination of magnitude, color and proper motion. The dependence on $N_D(\pi)$ leads to systematic bias in the mean parallax if one selected a sub-sample, S, from dataset D on the basis of π_o.

Lutz-Kelker corrections

$$\Delta M_{LK} \quad = \quad \langle M_{true} - M_o \rangle \quad = \quad \langle 5log\frac{\pi}{\pi_o} \rangle \tag{2}$$

provide a means of correcting this bias in the absolute magnitude plane. The bias is not present if there is no selection based on π_o, as in the methods of mean parallaxes (e.g. averaging open cluster parallaxes) or reduced parallaxes (cf. Feast & Catchpole's (1997) Cepheid analysis and

Feast (2000)). The LK bias, however, is always present when one averages absolute magnitudes, since the latter cannot be calculated if π_o is negative.

Lutz & Kelker computed ΔM_{LK} for the specific case of a uniform distribution, $N_D(\pi) \propto \pi^{-4}$, and are limited to $\frac{\sigma_\pi}{\pi} < 0.175$. Hanson (1979) showed that common observational selection effects (magnitude limits, proper motion limits) lead to less steep power-law density distributions, and used series expansion to derive general solutions for $N_D(\pi) \propto \pi^{-n}$. This results in both smaller LK corrections, and reliable corrections for higher values of $\frac{\sigma_\pi}{\pi}$ (see also Koen, 1992).

With an apparent magnitude limit of $V \sim 12$, the Hipparcos dataset is magnitude-limited for stars with $M_{true} > 5.0$. In that case, the power-law exponent n of the density distribution and the resultant Lutz-Kelker bias are reduced significantly (Lutz, 1983), since imposing a magnitude limit modifies $N_D(\pi)$ without direct reference to π_o. The situation is analagous to observations toward an opaque molecular cloud at π_{MC}: no stars have $\pi < \pi_{MC}$, reducing the number of stars with smaller π, and the probability that, for any given star, $\pi < \pi_o$. This emphasises that there is no unique ΔM_{LK} for a given star: the correction depends on context. If one modifies $N_D(\pi)$ based on parallax-independent criteria before selecting the π-defined subsample, one also modifies ΔM_{LK}.

Effects on small angular scales

The surface density of Hipparcos targets was set to match the limits of the observing mode. As a result, the same objects were generally observed on successive scans of a particular region. This leads to correlations in the derived astrometric data over scales of up to ≈2 degrees (twice the field of view). One notable effect is that the precision of the mean parallax of stars with separations within this régime is $\frac{\sigma_\pi}{n^{0.35}}$ rather than $\frac{\sigma_\pi}{n^{0.5}}$ (Lindegren, 1988).

These correlations *may* lead to systematic bias in π_H at those angular scales. A comparison between the results from NDAC and FAST (Hipparcos catalogue, ESA, 1997; vol 3, ch 16 & 17) shows that differences of up to ~ 2 mas can occur within 2×2 degree regions near the ecliptic, corresponding to potential offsets of ≈ 1 mas in the final, merged catalogue. This result does not contradict the finding that the *global* zeropoint in π_H is reliable at the 0.1 mas level, but it serves a cautionary note for studies which require sub-milliarcsecond accuracy over 1-2 degree scalelengths.

Temporal effects in parallax measurement

In simple terms, the aim of the Hipparcos data reduction is to solve the following equations of condition for each target:

$$X = X_0 + \mu_X\,(T - T_0) + F_X\,\pi \tag{3}$$

$$Y = Y_0 + \mu_Y\,(T - T_0) + F_Y\,\pi \tag{4}$$

where (X, Y) are the observations, (X_0, Y_0) the co-ordinates, (μ_X, μ_Y) the proper motions and (F_X, F_Y) the parallax factors. If observations are not well-distributed in time, the unknowns are correlated. Hipparcos observations span the period January, 1990 to March, 1993, but no data were obtained between September and November, 1992, due to the loss of a gyro and subsequent re-configuration of the control system. As a result, January to March scans are available at four epochs, but September to November at only two. This imbalance leads to correlation coefficients, ρ, of up to ± 0.6 (Hipparcos catalogue, ESA, 1997; volume 1, ch 3.2), particularly in $\rho(\pi, \alpha)$. Ground-based parallax analyses almost always achieve $\rho < 0.1$ since one of the usual criteria is equal numbers of morning and evening observations. The existence of such high correlations does not guarantee bias, but the data are clearly vulnerable to such effects.

3. Distances to open clusters

The typical Galactic open cluster is populated by from a few tens to a few hundred stars, the product of a single star-forming region, spanning a narrow range in age and in chemical composition. Several fiducial clusters fall within the range of Hipparcos (Mermilliod et al, 1997; van Leeuwen et al, 1997). Since open clusters have a small line-of-sight depth and since cluster membership can be decided based on photometric, proper motion or radial velocity criteria, individual parallax measurements can be combined without incurring significant Lutz-Kelker bias, although other systematic sources of error may be present. In particular, the small angular size of the more distant clusters renders the astrometry susceptible to the small-scale systematic problems outlined in section 2. Indeed, Lindegren (1988) identified observations of open cluster stars as a powerful diagnostics of the extent of biases on small angular scales.

3.1. The Hyades

The metal-rich Hyades is near enough to permit ground-based trigonometric and, in resolved binaries, orbital parallax measurements, as well as statistical convergent-point analysis of the proper motions and radial velocities. The most recent latter study, by Schwann (1991), derived a mean modulus of 3.40±0.04 mag. (47.9±0.9 pc.) based on 145 stars with proper motion measurements from the FK5/FK4Sup, N30 and PPM catalogues. Perryman et al (1998) have analysed the Hipparcos astrometry, complemented by additional radial velocity data. Conventional convergent-point analyses derive the cluster distance from the equation

$$\bar{d} \quad = \quad \Sigma_i^N \left(\frac{V_S sin\lambda_i}{\kappa\mu_i}\right) \quad / \quad N \tag{5}$$

where $\kappa = 4.74$, V_S is the cluster space velocity, μ_i the individual proper motions toward the convergent point and λ_i the angular distance between each star and the convergent point. As Perryman et al point out, the exact location of the last parameter depends on the extent to which one allows for random cluster motions ($\sigma_{cl} \sim 0.2$ to 0.4 kms^{-1}) in defining the membership list. The Hipparcos data provide full positional and velocity information, and allow iterative membership analysis. Following that approach, Perryman et al derive a distance of 46.34±0.27 pc. ((m-M)=3.33) to the center of mass defined by 134 stars within a radius of 10 parsecs of the cluster center.

The main source of the 3.4% discrepancy between the Hipparcos result and Schwan's analysis is the value adopted for the cluster space motion: Schwan's datum is $V_S = 46.6\text{kms}^{-1}$, based on Detweiler et al (1984), while Perryman et al derive $V_S = 45.72\text{kms}^{-1}$ from CORAVEL data, a 2% difference. Most of the remaining discrepancy rests with the proper motions, and those differences are also responsible for the larger mean distance derived by Torres et al (1997) based on precise orbital parallax determination. Thus, the new Hyades distance determination is fully consistent with previous observations.

3.2. The Pleiades and other clusters

The same consistency with previous work is not apparent in initial analyses of the distance to the Pleiades cluster, which offered potentially the most significant result of the Hipparcos mission. The concensus of pre-Hipparcos studies located the Pleiades at a distance of $\sim$ 130pc., $(m\text{-}M)_0$=5.6 mag. However, both van Leeuwen & Hansen-Ruiz (1997) and Mermilliod et al (1997) derive a mean parallax from Hipparcos observations of $\bar{\pi} = 8.6 \pm 0.24$ mas, or r=116±3 pc. and $(m\text{-}M)_0$=5.33±0.05 mag., placing the (solar-abundance) Pleiades main-sequence $\sim$0.2 magnitudes fainter than the relation defined by nearby field stars ($\langle [Fe/H] \rangle \sim -0.15$ dex). Such a result can be accommodated within standard stellar evolution models, but only at the expense of invoking substantial anomalies, such as a helium abundance $Y_{MS} \sim 0.35$, and casting severe doubt on the global utility of distance determination by main-sequence fitting.

Pinsonneault et al (1998) re-examine this issue and show that plotting parallax against the $\rho(\pi, \alpha)$ correlation (see section 2) for individual Pleiads reveals a clear trend, with stars having higher $\rho(\pi, \alpha)$ also having larger π (their figure 18). As noted in section 2, observations with high $\rho(\pi, \alpha)$ correlation indices *may* also have biased parallax determinations. Since the relevant Pleiads are also predominantly bright stars near the cluster center, carrying most of the weight in deriving $\bar{\pi}$, the small angular-scale correlation inherent in Hipparcos astrometry leads one to expect correlated bias. Given that Pleiads with $\rho(\pi, \alpha) < 0.2$ give $\bar{\pi} = 7.49 \pm 0.50$mas, $(m\text{-}M)_0$=5.63±0.14 mag, and that there is an absence of any [Fe/H]$\sim$ 0 field stars which reproduce the van Leeuwen/Mermilliod main-sequence (Soderblom et al, 1998), it is reasonable to reject the initial Pleiades distance estimates as likely to be biased. The current best estimate of the distance of the Pleiades remains at $(m\text{-}M)_0$=5.6 magnitudes, or 132 parsecs (although see van Leeuwen, 1999, for a dissenting viewpoint).

Mermilliod et al (1997) and Robichon et al (1997) estimate distances to other nearby clusters, including Coma, Praesepe, IC 2602 and α Persei. Most are significantly more distant than the Pleiades and, in general, the Hipparcos distance moduli are consistent with previous determinations. An exception is the sparse, nearby cluster Coma Berenices, where Pinsonneault et al find a discrepancy of $\sim$ 0.2 magnitudes with respect to isochrone-fitting, and trends in $(\pi, \rho(\pi, \alpha))$ similar to those in the Pleiades.

In summary, Hipparcos astrometry does not provide the major challenge to stellar evolution theory suggested by the preliminary analyses. Systematic biases, correlated over scales of < 1 degree, limit the reliability of results derived for most open clusters. To echo Pinsonneault et al, it seems more prudent to regard these comparisons as tests of small-scale zeropoint errors, rather than as measurements of cluster distances.

4. The HR diagram defined by field stars

The technique of distance determination through main-sequence fitting rests on the hypothesis that the absolute magnitude (luminosity) of normal, single stars of a given color (effective temperature) is a monotonic function of metallicity. Hipparcos provides the first opportunity for a thorough empirical test of that hypothesis.

4.1. The abundance scale

In principle, fine analysis of high-resolution optical spectra, coupled with accurate temperature determination, provides the best basis for measuring stellar metallicity. However, it is only recently that such studies have been extended to significant numbers of even moderately faint stars. As a result, most investigations of abundance distributions are based on a variety of lower-resolution spectroscopic or photometric techniques, each anchored to the high-resolution scale through a limited (and non-unique) set of standards. The latter step can lead to systematic zeropoint offsets between different studies, particularly given the relatively-recent revision in the accepted value of the solar iron abundance (Biémont et al, 1991).

Advances in atmosphere modelling are opening the door for the first quantitative abundance analyses of late-type (K, M) dwarfs, notably using metal hydride bandstrengths (Allard et al, 1997; Gizis, 1997). However, most investigations continue to concentrate on F, G and early-K stars on the upper main-sequence. Sandage & Eggen (1959) originally devised δ(U-B), the ultraviolet excess index, as a means of using Johnson broadband photometry to measure relative line-blanketing shortward of 4000Å. Intermediate-band systems, such as Strömgren or Geneva photometry, have refined that measurement to some extent, while spectroscopic calibrations center on Fe, CH, CN and Mg features in the 4000-5300Å range (Rose, 1991; Carney et al, 1994; Jones et al, 1996).

Two of the most extensive abundance catalogues are Schuster et al's (1993) Strömgren-based dataset and Carney et al's (1994: CLLA) spectroscopic calibration. Schuster & Nissen (1989: SN) derive relations, tailored for main-sequence stars, between the (b-y), c_1 and m_1 indices and [Fe/H], while the CLLA calibration is based on high dispersion, but low signal-to-noise, spectra covering $\sim 50\AA$ centerd on the Mgb triplet. Abundances are derived by cross-correlating the latter spectra against observations of standard stars. Jones et al (1996) adopt a similar approach, basing their calibration on the CLLA system, while Flynn & Morell (1997) have devised an abundance index for G and K dwarfs which combines Geneva photometry with a Cousins (R-I)-based temperature scale.

All of these calibration (save the last) are tied to standards with high-resolution abundance analyses which predate the revision in $[\mathrm{Fe/H}]_\odot$. This leads to an offset between those abundance scales and metallicities defined in the more recent high-resolution studies by Axer et al (1994: AFG) and Gratton et al (1997a: GCC), while there are further systematic differences between the individual datasets. Reid (1998) finds

$$[Fe/H]_{GCC} \quad \sim \quad [Fe/H]_{AFG} \quad \sim \quad [Fe/H]_{SN} + 0.15 \quad \sim \quad [Fe/H]_{CLLA} + 0.3$$

with dispersions of $\sigma \sim 0.2$ dex. The offsets in the latter two scales become less pronounced at near-solar abundances. There is also evidence for a color term (temperature scale difference) between the Schuster & Nissen and Carney et al calibrations, while Axer et al clearly underestimate log$g$ for a number of Hipparcos stars (see also Nissen et al, 1997). Clementini et al (1999) generally confirm these offsets,

$$[Fe/H]_{GCC} = [Fe/H]_{SN} + 0.102 \pm 0.012$$

$$[Fe/H]_{GCC} = (0.935 \pm 0.032)[Fe/H]_{CLLA} + 0.181 \pm 0.173$$

while comparison with data from Ryan & Norris (1991) gives

$$[Fe/H]_{GCC} = [Fe/H]_{RN} + 0.40 \pm 0.04$$

Since the Jones et al scale is based on CLLA standards, one expects similar systematic errors in their abundances.

4.2. The HR diagram of the local disk

Stars within the immediate Solar Neighbourhood can be used to probe the general properties of the disk, since the overall velocity dispersion permits stars born at Galactic radii from 3 to 13 kpc to migrate through the Solar Radius. However, one of the early results from the Hipparcos survey was an indication that a significant fraction of the stars included in the most recent incarnation of the Nearby Star catalogue (CNS3: Jahreiss & Gliese, 1991) are not, in fact, within the nominal distance limits. analysis of the final catalogue confirms that $\sim$ 40% of the CNS3 stars observed by Hipparcos lie beyond 25 parsecs. This has obvious implications for statistical investigations which require unbiased, volume-limited samples. For example, figure 2 plots Hipparcos data for 106 nominally-single stars from the "G-dwarf" sample which are used by Wyse & Gilmore's (1995) to analyse the disk abundance distribution. Approximately 10 percent of the stars lie well above the main-sequence, and are likely to be evolved subgiants rather than dwarfs, while a further 5-10 stars are probably previously-unrecognised binaries. To date, no comparable study has been undertaken based on a volume-limited sample drawn from the Hipparcos catalogue.

While the Wyse/Gilmore stars do not constitute a volume-limited sample, these observations can be used to examine the variation in main-sequence location with changing abundance. Wyse & Gilmore use Strömgren photometry (from Schuster & Nissen, 1989) to estimate metallicities. Dividing the stars into four subsets, figure 2 compares the (M_V, (B-V)) distribution against 1-Gyr and 5-Gyr isochrones for solar abundance and [Fe/H]=-0.4 dex as computed by Bertelli et al (1994). Ignoring evolved stars, the relative ranking is consistent with expectations, with M_V generally becoming fainter with decreasing $[Fe/H]_{SN}$ at a given color. However, there is a systematic offset with respect to the isochrones, in the sense that the lower-abundance stars are brighter than expected given the Strömgren metallicity estimates. This is consistent with the abundance-scale comparisons given in the previous section.

The data plotted in figure 2 are consistent with the hypothesis of a monotonic change in the location of the main-sequence with varying metallicity. Moreover, the comparison with the isochrones suggests that most disk stars have abundances within ±0.2 dex of the solar value (see also figure 4 of Pinsonneault et al, 1998). Jimenez et al (1998) find a comparable systematic offset between the lower-abundance (-0.6 $< [Fe/H] < -0.4$) stars in the Flynn & Morell sample and their [Fe/H]=-0.5 isochrones. The implication is that previous studies, such as Wyse & Gilmore's analysis, overestimate the extent of the metal-poor tail to the disk abundance distribution, an inference consistent with Reid's (1998) analysis of Hipparcos data for Lowell proper-motion stars. Definitive results await more extensive observations, particularly detailed abundance determinations, of an Hipparcos-based volume-limited sample.

4.3. The HR diagram for halo subdwarfs

The low space density of the local halo coupled with the apparent magnitude limits of the Hipparcos survey lead to the final catalogue including only a few tens of metal-poor subdwarfs or subgiants with parallaxes of even moderate accuracy. As a result, those data offer only weak constraints on theoretical calculations. Cayrel et al (1997) compare the observed (M_{bol}, log T_{eff}) distributions for stars with $-1.8 < [Fe/H] < -1.2$, with temperatures taken from Alonso et al (1996), against (as-yet unpublished) isochrones computed by Lebreton and Vandenberg[1] They find a systematic offset of 0.01 in logT_{eff}, in the sense that the models are too hot. Adjusting the isochrones, Cayrel et al deduce an age of $\sim$ 14 Gyrs for the field halo, although it should be noted that that result rests on the location of two subgiants.

Figure 3 matches D'Antona et al's (1997) theoretical isochrones for 12 Gyr-old populations against data for subdwarfs from the AFG and GCC analyses, restricting the latter to stars with no known binary companion having $\Delta m < 4$ mag., with $\frac{\sigma_\pi}{\pi} < 0.15$ and with [Fe/H]< -0.7.

[1]As discussed further in section 5, the D'Antona et al (1997) models predict a similar (M_{bol}, log T_{eff}) relation for main-sequence stars with $M_V > M_V(TO)_1$.

As with the disk stars, the overall trend matches theoretical expectations. At metallicities exceeding [Fe/H] = -1.7 there is reasonable agreement between the observations and the predicted isochrones, a circumstance also noted by Chaboyer et al (1998). There is a suggestion that the lowest-abundance subdwarfs are more luminous (redder?) than expected, but this may reflect small-number statistics or an inherent selection effect rather than intrinsic stellar properties.

These data can also be used to estimate $\frac{\Delta Y}{\Delta Z}$, the proportional increase in helium and heavy element abundance due to stellar nucleosynthesis - an important quantity in determining the primordial helium abundance, Y_P. Helium abundance cannot be measured directly for stars on the lower main-sequence, but can be inferred by matching the observed distribution in the (M_{bol}, log T_{eff}) plane against theoretical isochrones. Based on pre-Hipparcos data for nearby disk G-dwarfs, Fernandes et al (1996) deduce that $\frac{\Delta Y}{\Delta Z} > 2$. Pagel and Portinari (1998) extend this analysis by matching Hipparcos data for stars in the abundance range[2] $-3 < [Fe/H] < 0$ against isochrones computed for $\frac{\Delta Y}{\Delta Z} = 0, 3, 6$. Limiting analysis to stars with $M_V > 5.75$, Pagel & Portinari deduce a best-fit value of $\frac{\Delta Y}{\Delta Z} = 3 \pm 2$, with the large uncertainty reflecting primarily the small sample size.

5. Distances to globular cluster

While globular clusters lie well beyond the scope of present parallax measurement, high-accuracy astrometry which Hipparcos provides for metal-poor stars allow re-examination of the cluster distance scale through indirect techniques, notably main-sequence fitting. In particular, new data for field subdwarfs offer the chance to retrace the observer's route to globular cluster distances (Sandage, 1970; 1986). A pre-requisite for the successful application of those techniques is a consistent metallicity scale for both clusters and field stars.

5.1. Cluster abundances

The most-frequently referenced source of cluster metallicities remains the extensive study by Zinn & West (1984). Their calibration is based on large-aperture broad- and narrow-band photometry, with individual magnitudes combined to give reddening-free color indices; and on integrated low-resolution spectrophotometry, isolating the Ca II K-line, G-band and Mgb features. Those measurements are scaled and averaged to give a composite estimate of the Q_{39} index, measuring the line-blanketing in the 3820-4010 Å region. That index was calibrated itself in terms of [Fe/H] using Cohen's (1983) analysis of high-resolution, image-tube spectra of giants in sixteen clusters.

Cohen's observations were, of necessity, limited to stars near the tip of the red-giant

[2]Note that the stellar abundances are drawn either from Carney et al (1994) or the compilation by Cayrel de Strobel et al (1997), and can differ by 0.2-0.3 dex with more recent analyses.

branch. Advances in detector technology over the last decade have allowed high signal-to-noise, high-resolution spectroscopy of larger samples of cluster giants, notably by the Lick/Texas group (Sneden et al, 1997 and refs within: hereinafter LT) and by Gratton and co-workers (Carretta & Gratton, 1997, and refs within: CG97). Both of the latter groups tie their analyses to the revised value of the solar iron abundance, adopting log ϵ(Fe)=7.52, $\sim$ 0.15 dex lower than the previously-accepted value. The LT analysis, aimed primarily at determining [O/Fe] ratios, spans stars in seven clusters (Table 1), with homogeneous observations, temperatures derived from either (B-V) [M15, M92] or (V-K) colors, using MARCS model atmospheres (Gustafsson & Bell, 1979) as a reference.

Carretta & Gratton analyse both their own CASPEC echelle spectra and equivalent-width data from the literature, including the LT dataset. Temperatures are based primarily on (V-K) colors, while CG97 adopt the Kurucz (1992) model atmosphere grid as their reference. The resulting abundances are $\sim$ 0.1 dex more metal-rich than previous analyses, including the LT determinations. CG97 ascribe this systematic discrepancy to the different model atmospheres used in the different studies (although one should note that JR King et al (1998) derive a *lower* abundance in their re-analysis of LT's M92 data).

Both LT and CG97 compute true iron abundance, [Fe/H], based on equivalent widths of Fe I and Fe II lines. As with field subdwarfs, population II globulars are expected to have non-solar elemental abundance ratios, with enhanced oxygen and α-elements. The LT observations, however, reveal more complex behaviour among the cluster giants than in the field, with [O/Fe] values ranging from +0.3 dex to < -0.4dex in some clusters (notably M13). [α/Fe] ratios are typically +0.2 to +0.3, typical of the halo. The oxygen abundance anomalies are coupled with an observed anti-correlation of Na-O and correlation of Na-N, and are probably explicable in terms of deep-mixing nucleosynthesis (Kraft et al, 1993), but possible inconstancy in the total CNO abundance may reflect primordial variations. The latter would represent a potential complication for MS-fitting. If [O/Fe]=+0.3 is adopted as the standard value for [Fe/H]< -1, then following Salaris et al (1993),

$$logZ \quad = \quad [M/H] \quad - \quad 1.66 \quad = \quad [Fe/H] \quad - \quad 1.45 \tag{6}$$

All of these analyses center on stars on the giant branch, whereas MS-fitting demands (by definition) matching cluster subdwarfs against field subdwarfs of comparable abundance. While there is no *a priori* reason to distrust the existing cluster [Fe/H] data, the variations in [O/Fe] emphasise the complications in dealing with evolved stars. Spectroscopy of main-sequence cluster members would allow abundance calibration using the same criteria as used in field-subdwarf calibration. Such observations are within the scope of the new generation of 8-metre class telescopes and are underway (J. Cohen, priv. comm.), but no studies have been completed. JR King et al (1998) have obtained the first high-resolution spectra of six subgiant stars near the M92 turnoff. Their analysis of those data, based on the Kurucz (1992) atmospheres and with temperatures estimated from (B-V) colors, imply [Fe/H]~ -2.5, significantly lower than either the

LT or CG97 analyses, but matching Peterson et al's (1990) earlier analysis of two M92 red giants. One should note, however, that they derive a higher reddening (E_{B-V}=0.07) than any other study, suggesting possible systematic errors in the colors and the temperature scale. Observations of a larger sample of stars, preferably with accurate infrared colors, in this and other clusters should be given high priority.

5.2. Cluster distances

Empirical main-sequence fitting, the observer's route to cluster distances, is simple in principle. Observations of nearby stars with known trigonometric parallax are used to define the location of the main-sequence in the absolute magnitude/color plane; photometry of cluster stars allows one to determine a fiducial cluster main-sequence in the apparent magnitude/color plane; and the offset between the two sequences is the distance modulus of the cluster. In practise, this idealised concept is vulnerable to a number of complications.

1. Photometry: the field-star and cluster observations must both be of high accuracy and tied to a consistent photometric system. Crowding is clearly a problem in analysing cluster data, although the high spatial resolution offered by the Hubble Space Telescope (HST) addresses that issue. Most field subdwarfs have photometry in only the Johnston B and V passbands, and individual (B-V) measurements drawn from the literature can differ by up to 0.04 magnitudes. Since the slope of the main-sequence is $\frac{\partial M_V}{\partial (B-V)} \approx 5$, systematic uncertainties at that level lead to errors of up to 0.2 magnitudes in (m-M). Accurate, homogeneous UBVRIJHK photometry for both field and cluster subdwarfs is eminently desirable.

2. Abundances: the metallicity of the calibrating stars should be either close to that of the individual cluster under study, or the stellar parameters at least adjusted reliably to match the appropriate abundance. Variations in the [O/Fe] and [α/Fe] ratios from the nominal values of $\sim +0.2/+0.3$ amongst field subdwarfs (e.g. HD 134439 & 134440: King, 1997) further complicate this issue. The most recent stellar models (e.g. D'Antona et al, 1997) indicate $\frac{\partial (B-V)}{\partial [Fe/H]} \sim 0.14$ at [Fe/H]$= -1$ and $\frac{\partial (B-V)}{\partial [Fe/H]} \sim 0.05$ at [Fe/H]$= -2$for $M_V > 5$.

3. Binary and multiple stars: unrecognised duplicity can lead not only to erroneous absolute magnitude estimates for calibrating subdwarfs, but can distort the position of the fiducial (magnitude, color) relation for the lower main-sequence in binary-rich clusters, such as NGC 288 (Bolte, 1992).

4. Reddening: most clusters are subject to foreground Galactic obscuration, as are a few calibrating subdwarfs. Qualitatively, if the cluster reddening is *overestimated* (cluster sequence too blue), the distance modulus is also *overestimated*. On the other hand, if the reddening of the calibrating subdwarfs is *overestimated* (reference sequence too blue), the cluster distance is

underestimated.

5. Distribution in (M_V, color): even with the addition of Hipparcos data, few subdwarfs are available over the full range of M_V/(B-V) and [Fe/H]. Typically, the distance to a given cluster is estimated using only five to ten subdwarf calibrators, so decisions on whether to include individual field stars can influence the derived (m-M) by ~ 0.1 magnitude.

6. Evolution off the main-sequence: theoretical isochrones show that at ages of from 10 to 16 Gyrs, metal-poor ([Fe/H]<-1) stars within 1.5 magnitudes of the turnoff have luminosities which lie above the zero-age main-sequence, although the offset is less than 0.1 magnitude for $\Delta M > 1$ magnitude. This reduces further the potential number of calibrators. One should note, however, that evolution will bias MS-fitting to larger distances only if the calibrating field turnoff stars are significantly older (i.e. more luminous) than the cluster.

The pre-Hipparcos cluster distance scale

The sparse numbers of local subdwarfs with accurate ground-based parallax measurements discouraged purely-empirical MS-fitting analyses, and most pre-Hipparcos analyses either match model isochrones directly against cluster data (the theoretician's route to distances), or adopted a semi-empirical approach. In some studies (e.g. Richer & Fahlman, 1986) isochrones are used to adjust subdwarf colors to those appropriate to the cluster abundance, and the MS-fitting distance derived using the resultant mono-metallicity sequence; alternatively, the subdwarfs calibrate zeropoint offsets in the isochrones, and the latter are adjusted and matched to the cluster color-magnitude data. In one of the more influential studies, Bolte & Hogan (1995) adopted the latter approach in deriving the distance and age of M92, using data for HD 103095 (Groombridge 1830), to derive an offset of 0.015 magnitude in the (B-V) colors predicted by Bergbusch & Vandenberg's (1992 - BV92) models. Clearly, this single-point adjustment assumes that the models have no systematic errors as a function of luminosity and/or effective temperature (i.e. the isochrones have the correct shape in the color-magnitude plane).

Bolte & Hogan's results were not unchallenged. D'Antona, Caloi & Mazzitelli (1997 - DCM) derive a distance modulus of 14.80±0.1 to M92, based on weighted MS-fitting against eight nearby subdwarfs with accurate ground-based parallaxes, rather than relying on only Groombridge 1830. Distance estimates to the extreme metal-poor clusters M30 and M68 exceed previous analyses by a similar factor.

RR Lyrae stars provide an alternative to MS-fitting in cluster distance determination, and we discuss their luminosity calibration in section 6.3. The other main options are astrometric distances and, recently, white dwarf sequence fitting. In the former case, measurement of the proper-motion dispersion of cluster members is combined with observations of the radial velocity dispersion and a dynamical model to derive a distance estimate. This method has the advantage of being reddening-independent, but requires relative astrometry of extremely high precision. Rees (1997) has summarised results for eight clusters, and typical uncertainties are from ±0.2 to ±0.4 mag in $(m\text{-}M)_0$. As yet, those results offer only weak constraints on the distance scale.

Accurate photometry for white dwarfs in globular clusters has become possible only with the existence of HST. Deep imaging has led to the detection of degenerate sequences in at least three clusters: NGC 6752 (Renzini et al, 1996), NGC 6397 (Cool et al, 1996) and M4 (Richer et al, 1997). Renzini et al use their observations to estimate a distance modulus of 13.05 to NGC 6752, choosing as calibrators nearby disk white dwarfs with spectroscopic masses of $\sim 0.5 M_\odot$, close to the expected value for halo white dwarfs. The latter mass estimates, however, are based on white dwarf models with thin-hydrogen atmospheres: thick-hydrogen atmosphere models provide a better match to masses derived using gravitational redshifts (Reid, 1996a), and imply higher masses for these disk calibrators. Lower-mass white dwarfs have larger radii, and therefore higher luminosities at a given effective temperature, so Renzini et al are likely to have underestimated $(\text{m-M})_0$ in their analysis. Concordant with this hypothesis, Richer et al note an offset of 0.1 magnitude between their MS-fitting distance estimate to M4 (1.73 kpc - in good agreement with the astrometric estimate) and the WD-fitting result. Finally, Cool et al do not use their data to estimate directly a distance to NGC 6397, but inspection of their figure 6 shows a systematic offset of $\sim +0.3$ magnitudes between the $0.5 M_\odot$ theoretical white dwarf sequence and their data for the adopted $(\text{m-M})_0 = 11.7$ magnitudes.

Table 2 presents distance estimates, derived through these various techniques, for a representative sample of clusters. The 'standard' pre-Hipparcos distance scale is characterised using the values listed in Harris' (1996) compilation. In each case we list both the true distance moduli and the reddening, E_{B-V}, (from Harris). The latter values are derived using a variety of techniques, and as a self-consistent reference we list reddenings derived from Schlegel et al's (1998) 100 μm COBE/IRAS all-sky analysis. In general, increasing the adopted cluster reddening by ΔE_{B-V} leads to an increase of $2 \times \Delta\text{E}_{B-V}$ in $(\text{m-M})_0$. In addition, we list the apparent magnitude (uncorrected for reddening) at the main-sequence turnoff. Those values are taken from the fiducial cluster sequences referenced in Reid (1997, 1998).

Post-Hipparcos cluster distance determinations

Even with the completion of the Hipparcos catalogue, there are few lower main-sequence subdwarfs which are unambiguously single, have reliable abundance determinations and accurate parallaxes. Extreme metal-poor clusters, such as M92 and M15, are ill-served with calibrators for distance measurement. Table 2 lists distance modulus determinations from the several post-Hipparcos MS-fitting analyses Apart from the choice of abundance calibration and foreground reddening, each analysis employs a different set of subdwarf calibrators and uses different color-corrections and residual-minimisation techniques in MS-fitting. Uncertainties in $(\text{m-M})_0$ are at least ± 0.1 magnitude.

The largest discrepancies between the pre- and post-Hipparcos distance estimates listed in Table 2 lie among the extreme metal-poor clusters, notably M92, where Harris' distance modulus is 0.1 magnitude shorter than even Bolte & Hogan's result. Reid's (1997) initial Hipparcos analysis produces the largest distances, but, apart from being based on the Carney et al (1994) abundance scale, Pont et al (1998) point out that several of metal-poor calibrators used in that survey are binaries.[3] In their M92 analysis, Pont et al apply statistical corrections to adjust M_V for known binary subdwarfs, a procedure criticised by both Chaboyer et al (1998) and Reid (1998); excluding those stars increases their derived modulus to $(m-M)_0=14.74$, in close agreement with other recent studies.

NGC 6397 represents a special case. The pre-Hipparcos distance estimate rests on one subdwarf, HD 64090, whose parallax is reduced by 20% by Hipparcos astrometry. Lying at low latitude, this cluster is subject to significant field-star contamination, but deep HST observations span a sufficient baseline in time to allow proper-motion identification of members, and the resultant color-magnitude diagram extends to luminosities approaching the hydrogen-burning limit (IR King et al, 1998). Exploiting these results, Reid & Gizis (1998) have used nearby M-subdwarfs with accurate ground-based parallax data to undertake MS-fitting on the lower main-sequence, and derive a distance modulus of 12.12 ± 0.15.

Given a distance to NGC 6397, that cluster can be used as a template to estimate distances to more metal-poor systems by extending the differential upper-MS matching technique devised by Vandenberg et al (1990). Theoretical isochrones can be used to make explicit allowance for intrinsic abundance-dependent variations in the color and luminosity at the turnoff, corrections analagous to those required in constructing a mono-metallicity sequence of subdwarf calibrators. This requires that the models are accurate in a differential sense over a limited range in luminosity and effective temperature. The resultant distance estimates (Table 2 - from Reid & Gizis, 1998) are in good agreement with more direct analyses. Overall, MS-fitting based on Hipparcos subdwarf data points to a modest increase of 0.1 to 0.2 magnitudes in the distance moduli, or 5 to 7% in distance, of the majority of globular clusters.

5.3. Globular cluster ages

Much of the interest in globular cluster distances centers on their use as Galactic age indicators. The luminosity at the main-sequence turnoff remains the most effective absolute-age determinant, although there are observational difficulties in defining the parameter. The main-sequence is vertical near the turnoff, so M_V(TO) can be defined with a typical accuracy of only ± 0.1 magnitude, equivalent to an uncertainty of ~ 1.5 Gyrs in age. Matching M92 observations against the available stellar models, Bolte & Hogan set a firm lower bound of 16 ± 2 Gyrs on the age of the Galaxy, identifying a strong conflict between stellar evolution-based and (short distance-scale) cosmological estimates of the age of the Universe (see also Chaboyer et al, 1996). As in all classical drama, hubris stepped forth on cue, not only in the guise of a longer distance scale, but also in the form of refined physics of stellar interiors.

[3] Note that Reid (1997) derives $(m-M)_0=14.80$ for M92 based on pre-Hipparcos data, in good agreement with D'Antona et al, and $(m-M)_0=14.82$ by direct calibration against the metal-poor F-type subdwarf, HD 19445.

Main-sequence fitting based on Hipparcos-calibrated subdwarfs implies M_V(TO) values that are brighter by 0.1 to 0.15 magnitudes, corresponding to an age reduction of 1.5 to 2 Gyrs. However, revisions in the (M_V(TO), [Fe/H], age) relation lead to significant changes in the age calibration. The last decade has seen substantial improvement in defining many of the physical parameters underlying stellar interior theory, prompted primarily by theoretical inconsistencies revealed through helioseismological observations. In particular, while most model isochrones predating 1994 are based on the equation of state derived by either Eggleton et al (1973) or Straniero (1988), and opacities from the Los Alamos calculations (Huebner et al, 1977), recent calculations employ the new generation of OPAL opacity data (Rogers & Iglesias, 1992; Seaton et al, 1994; Iglesias & Rogers, 1996), and the corresponding equations of state (Rogers et al, 1996). The first extensive set of models to incorporate these new data were computed by Mazzitelli, D'Antona & Caloi (1995 - MDC; see also DCM), and those calculations predict significantly lower turnoff luminosities for a given age and abundance: there is a $\sim$ 0.2 magnitude ($\sim$ 3 Gyr) offset in M_V(TO) between the DCM calibration and the pre-OPAL Straniero & Chieffi (1991) models (figure 4a).[4] Matched against the DCM calibration (figure 4b), the Hipparcos-based distance scale implies cluster ages of 11 to 13 Gyrs.

Figure 4a shows that the BV92 models predict turnoff absolute magnitudes within 0.1 magnitude of the OPAL-based DCM calculations. This is due partially to the highly-enhanced [O/Fe] ratios adopted in the former models - both DCM and Straniero & Chieffi employ scaled-solar abundances. Given this concordance in M_V(TO), one might ask why Bolte & Hogan deduced an age of 16 Gyrs for M92. The answer lies with the second parameter of the color-magnitude diagram. Figure 5 compares 12-Gyr isochrones from BV92 and DCM for [Fe/H]=-2.26 and -2.03. respectively. The isochrones in (M_{bol}, log T(eff) are almost identical on the lower main-sequence, but diverge near the turnoff, with Bergbusch & Vandenberg predicting higher temperatures. However, there is a significant, luminosity-dependent color offset between the isochrones in the (M_V, (B-V)) observational plane. These discrepancies reflect several factors: different effective-temperature/color transformations; different bolometric corrections; different treatment of convection; and inclusion or exclusion of helium sedimentation. In the last context, Straniero et al (1997) demonstrate that allowing for helium diffusion in their OPAL-based models moves the turnoff redward by up to 0.06 magnitudes in (B-V). Matching their models directly against Walker's (1994) M68 data, they estimate $(m-M)_0$=15.10 (for E_{B-V} = 0.04 cf. Table 2) and an age of $\sim$ 13 Gyrs.

Clearly, even if one aims to use M_V(TO) as the age indicator, there is a strong tendency to select an isochrone which matches the observed color of the turnoff - particularly given the observational ambiguity in locating M_V(TO). Figure 5 shows that that choice drives one to choosing an older age if the BV92 isochrones are taken as the reference set than if one matches

[4]Calculations by Cassisi et al (1998),incorporating further modifications in the input physics, predict turnoff luminosities lower by $\Delta logL \sim 0.05$ than even the MDC calibration.

against the DCM calculations: the former predict an intrinsically bluer turnoff for a given age and composition. In general, the agreement in age estimates derived from M_V(TO) and full-CMD comparisons against OPAL-based stellar models favors cluster ages in the range 11 to 13 Gyrs.

5.4. Summary

The changes in the cluster distance scale resulting from the addition of accurate Hipparcos parallax data for halo subdwarfs are relatively minor: no more than 0.15 magnitudes, or $\sim$ 7% in distance. Nonetheless, when combined with the recent revisions in the physics of stellar interiors, the net result is a reduction of 30 to 40% in the likely ages of even the most metal-poor globular clusters. A final resolution of the age question must always rest with the stellar models, but the availability of accurate parallaxes for a larger number of unambiguously-single subdwarfs, particularly at [Fe/H]<-1.5, would go a long way toward setting distance estimates of a firm foundation. This requires sub-milliarcsecond astrometry to at least 15th magnitude, and probably the next astrometric space mission. In the interim, more accurate photometric and spectroscopic data for both subdwarfs and a larger number of globular clusters (including CCD photometry of stars *above* the turnoff) would not be amiss.

6. Distance indicators

6.1. Cepheid variables

The Cepheid period-luminosity (P-L) relation constitutes the backbone of the extragalactic distance scale. Descendants of intermediate-mass stars, Cepheids have typical ages of $\sim 10^8$ years and therefore are found predominantly near the parent star-forming region. As a result, only a handful of variables lie within 1 kpc. of the Sun, and most Cepheids are subject to considerable foreground reddening. However, the continued spatial association with coeval lower-mass stars offers a potential means of distance determination, albeit for a limited number of stars. Until recently, the primary calibrators of the Galactic P-L relation were thirteen Cepheids in clusters and associations (Sandage & Tamman, 1968), whose distances were estimated using main-sequence fitting. More recent calibrations of the same kind are by Feast & Walker (1987) and Laney & Stobie (1994) (see later). Theoretical models (e.g. Chiosi et al, 1993) predict a small metallicity-dependence in M_{bol}, which is amplified by differential blanketing at optical wavelengths. Metal-rich Cepheids are cooler and brighter in V and I. The amplitude of variation is currently under debate (Sasselov et al, 1997; Kochanek, 1997; Sandage, Bell & Tripicco, 1999), but since M31 Cepheids are near-solar abundance and LMC Cepheids have [O/H]~ -0.3 ($\delta M_V \sim -0.05$), we consider this effect no further.

Hipparcos astrometric analyses

Observations of over 200 Galactic Cepheids are included in the final Hipparcos catalogue, with most lying at distances exceeding 1 kiloparsec. As a result, few variables have parallaxes measured to an accuracy of better than 2σ. Lynga & Lindergren (1998) estimate parallaxes for two Cepheids associated with open clusters, but with accuracies of no better than 40%. However, since the Hipparcos Cepheids were not selected for observation based on parallax, the sample as a whole is amenable to statistical analysis. Feast and Catchpole (1997) have used the method of reduced parallaxes to complete the most rigorous such study to date.

Given parallax data for an unbiased sample of stars at effectively the same distance (e.g. open cluster members), $\langle\pi\rangle = \Sigma\frac{\pi_i}{N}$. Consider an unbiased (as regards π) sample of stars spanning a range of distances with identical, but unknown, M_V. The apparent magnitude can be used to scale each parallax measurement to a single distance, e.g. $\pi_i' = \pi 10^{-0.2\times V_0}$, and $\langle\pi'\rangle = \Sigma\frac{\pi_i'}{N}$ gives the appropriate zeropoint. Cepheids do not have identical magnitudes, but follow the P-L relation

$$\langle M_V\rangle \quad = \quad \delta logP \quad + \quad \rho$$

which can be used as a scaling relation. Feast and Catchpole adopt $\delta = -2.81$ from Magellanic Cloud Cepheid data, and solve for ρ using

$$10^{0.2\rho} \quad = \quad 0.01\pi 10^{0.2(\langle V_0\rangle - \delta logP)}$$

The Cepheid period-color relation is used to estimate foreground reddening, and hence $\langle V_0\rangle$, for each star. Since Cepheids follow a period-luminosity-color (PLC) relation, the P-L relation has intrinsic scatter. However, the slope of the color dependence in (B-V) (~ 2.5) is close to the ratio between total and selective reddening (~ 3.15). Thus, using the period-color relation to estimate E_{B-V} compensates for a substantial proportion of the intrinsic scatter in the P-L relation. Feast and Catchpole derive $\rho = -1.43 \pm 0.1$.

Feast & Whitelock (1998) follow similar precepts to derive the zeropoint, ρ_2, of the PLC relation as $\rho_2 = -2.38 \pm 0.1$. This calibration allows the derivation of Galactic rotation constants from proper motion data, and Feast and Whitelock good agreement with radial velocity analyses. Inverting the process, they note that Pont et al's (1997) Galactic rotation study implies $\rho_2 = -2.42 \pm 0.13$.

Madore & Freedman (1998) and Oudmaijer et al (1997) have criticised the Feast/Catchpole analysis and derive zeropoints fainter by ~ 0.1 magnitude. However, both calibrations are based on variables with higher-accuracy Hipparcos parallaxes; that is, the samples are parallax-selected, and therefore liable to bias. Oudmaijer et al apply estimated Lutz-Kelker corrections to individual stars, but the substantial values of $\frac{\sigma_\pi}{\pi}$ mean that those corrections are sensitive to the assumed spatial distribution. In contrast, the individual weights in the Feast/Catchpole reduced parallax analysis are determined primarily by the apparent magnitude, rather than π, giving an estimate of ρ which is effectively unbiased by parallax uncertainties (Feast, Pont & Whitelock, 1998).

The highest-weight Cepheids in the Feast/Catchpole analysis have near naked-eye apparent magnitudes, significantly brighter than the average amongst stars used to test the Hipparcos absolute zeropoints, and the possibility of low-amplitude magnitude terms has not yet been eliminated fully. However, Sandage & Tamman (1998) point out that Feast & Catchpole's P-L calibration is no more than 0.1 magnitudes brighter than previous Galactic calibrations, notably their 1968 cluster-Cepheid calibration (with the cluster distances given by Kraft's (1961) main-sequence fitting). Those discrepancies lie at the 1σ level, even without allowing for possible unrecognised systematics in the Hipparcos analysis.

Pulsational parallax analyses

The concept of using Cepheid radial pulsations to estimate distances originated with Baade (1926) and was elaborated further by Wesselink (1946). In the simplest terms, the difference in apparent magnitude at phases with identical colors (temperatures) is interpreted as a difference in angular size; integrating over the velocity curve gives the corresponding change in linear diameter; and the distance follows from the ratio of those quantities. analysing the velocity curve requires correcting the observed velocities, integrations over the full stellar disk, to give pulsational velocities. Recent studies are based primarily on variations on the surface-brightness method introduced by Barnes & Evans (1976), who derived a linear relation between visual surface brightness, S_V, and Johnson (V-R) color. The technique has been extended to near-infrared colors (cf. Di Benedetto, 1997), with the zeropoints for these relations set through observations of non-variable stars, generally late-type giants, whose diameters can be measured directly using interferometric techniques (Fouqué & Gieren, 1997).

The most recent analyses are by Di Benedetto (1997), based on an (S_V, $(V\text{-}K)_0$) calibration, and Gieren et al (1997, 1998), who use both (S_V, $(V\text{-}K)_0$) and (S_K, $(J\text{-}K)_0$) relations. Gieren et al (1996 and refs within) have also applied an (S_V, $(V\text{-}R)_0$) to analysis of individual Cepheids associated with Galactic open clusters and associations. Comparing the derived distances, Di Benedetto finds excellent agreement between his Baade-Wesselink estimates and main-sequence fitting distances (from Feast & Walker, 1987, and Laney & Stobie, 1994) for cluster Cepheids: 25 variables give

$$\Delta\mu_0 \quad = \quad (m-M)_0^{DB} \quad - \quad (m-M)_0^{ZAMS} \quad = -0.05 \pm 0.23$$

All of these studies are based on a Hyades distance modulus of 3.27, and hence the zeropoint should be made brighter by 0.06 magnitudes to match the Hipparcos analysis (Perryman et al, 1998). Comparison between the Di Benedetto and Gieren et al analyses (17 stars in common) gives

$$\Delta\mu_0 \quad = \quad (m-M)_0^{DB} \quad - \quad (m-M)_0^{GFG} \quad = 0.01 \pm 0.21$$

Many of these Cepheids have substantial foreground reddening: ten of the 34 stars in Gieren et al's sample have $E_{B-V} > 0.5$ mag., while only three have $E_{B-V} < 0.25$ magnitudes. Thus, the deduced M_V is subject to uncertainties in both E_{B-V} and in R, the ratio of total to selective absorption. [5] In general, the slope (δ) adopted for the period-luminosity relation is taken from observations of LMC variables. Gieren et al derive $\delta = -2.76$, $\rho = -1.29$, a relation less steep than the Laney & Stobie LMC calibration, and 0.16 fainter than Feast & Catchpole's relation at logP = 0.5, and 0.2 magnitudes fainter at logP = 1.5. Di Benedetto finds an intermediate zeropoint (again adjusted to $(m\text{-}M)_{Hyades}$=3.33) of $\rho = -1.41$ from his analysis of Galactic Cepheids.

6.2. Red clump stars

Population II horizontal branch stars are at the core-helium/H-shell burning stage of evolution. Their higher-abundance counterparts form the 'red clump' evident on the giant branch in intermediate-age disk open clusters, such as NGC 2420 and 2243, and in the field population of the Galactic Bulge and the Magellanic Clouds. Hipparcos provides the first accurate definition of the Solar Neighbourhood population, with over 1000 evolved stars having both $\frac{\sigma_\pi}{\pi} < 10\%$ and BVI photometry. analysing that sample, Paczyński and Stanek (1998) derive $\langle M_I \rangle = -0.185 \pm 0.016$, with the majority of the clump stars lying in the range $0.85 < (V-I)_C < 1.1$, $-0.4 < M_I < 0.1$.

Paczyński & Stanek propose using these stars as distance indicators. Neither the Solar Neighbourhood stars nor the Bulge population ($1.0 < (V-I)_C < 1.4$) show evidence for significant trends in $\langle M_I \rangle$ with color. Bolstered by evolutionary models (Jimenez et al, 1998), and despite the near-solar abundance derived McWilliam & Rich (1994), the difference in mean colors is interpreted as a metallicity effect. The invariance in $\langle M_I \rangle$ then implies at most a weak dependence on abundance. Building on that inference, Udalski et al (1998) extend analysis to the Magellanic Clouds.

The lynchpin of this technique is the assumption that, over the age range $\sim 2-10$ Gyrs, $\langle M_I \rangle$ is invariant with metallicity. However, Cole (1998), Girardi et al (1998) and Beaulieu & Sackett (1998) show that evolutionary models predict that red clump stars spanning a range of $\delta I \sim 0.5$ magnitudes, depending on age and abundance. Cole, in particular, points out that the small dispersion in M_I within individual systems can be understood as reflecting internal homogeneity, rather than global uniformity. Moreover, contrary to expectations, Paczyński (1998) finds that individual Bulge stars show no correlation between (V-I) and [Fe/H] (assessed from Washington photometry). Finally, one should note that none of the stellar models used in these analyses are based on the new OPAL opacities, rendering the relative zeropoints uncertain. Given these complications, and the lack of consistency with other distance indicators, it is prudent to defer full acceptance of red clump stars as distance indicators until a reliable independent calibration has been obtained.

---

[5] These considerations are of lesser importance an near-infrared wavelength. Extensive JHK observations of both Galactic and Magellanic Cloud Cepheids are being undertaken by SE Persson and collaborators.

6.3. RR Lyraes and blue horizontal branch stars

Although less luminous than Cepheids, RR Lyraes are identifiable in most Local Group galaxies, providing an independent test of the distance scale. The most common, and most easily identified, are the Bailey RRab-type fundamental-mode pulsators, with asymmetric, large-amplitude (ΔV ~1 mag) light curves. First-overtone RRc-type variables have near-sinusoidal light curves, $\Delta V \sim 0.4$mag, while a growing number of double-mode RRd-type stars and a few second-overtone RRe-type variables are being identified, primarily through high-accuracy CCD photometric monitoring of globular clusters. Discrepancies persist, however, amongst the various techniques used to calibrate the mean luminosity of both variable and non-variable horizontal branch stars, centering particularly on the metallicity dependence (see Smith, 1995). While only a subset of those analyses rely directly on astrometry, we review recent results from each method to set the Hipparcos-based results in context.

Direct trigonometric parallax measurements

Like Cepheids, RR Lyraes have short evolutionary lifetimes ($\tau \sim 10^8$ years) and the local space density is correspondingly low ($\sim 2 \times 10^{-8}$ stars pc^{-3}). Indeed, the eponymous star of this class (RR Lyrae) is the only star with an Hipparcos parallax determined to a precision better than 15% ($\pi = 4.38 \pm 0.59$ mas), implying an uncorrected absolute magnitude of M_V=$0.82^{+0.28}_{-0.31}$ at [Fe/H]=-1.37. Both de Boer et al (1997) and Gratton (1998) have analysed Hipparcos astrometry of larger samples of field horizontal branch stars. de Boer et al note that the eight blue horizontal branch (BHB) stars in their sample have individual absolute magnitudes in agreement with Dorman's (1992) model predictions, although the inferred masses are only $\sim 0.4 M_\odot$, significantly lower than expected. Gratton estimates a mean absolute magnitude for his larger sample of 22 stars using a variation of the reduced parallax method, with the M5 horizontal branch taken as a template of the absolute magnitude distribution. He derives a mean absolute magnitude of $\langle M_V \rangle = 0.69 \pm 0.1$ for $\langle [Fe.H] \rangle = -1.4$. Finally, Tsujimoto et al (1998) have analysed data for 125 RR Lyraes ($-2.5 < [Fe/H] < 0.06$) using the maximum likelihood technique proposed by Smith (1988), and derive

$$M_V(RR) \quad = \quad (0.59 \pm 0.37) \quad + \quad (0.20 \pm 0.63)([Fe/H] + 1.60) \tag{7}$$

Statistical parallaxes

The mean absolute magnitude of a kinematically-distinct group of stars can be estimated using statistical methods if one has radial velocity and proper motion data (and photometry) for a representative sample, and field RR Lyraes are well suited to this type of analysis. Most studies are based substantially on stars drawn from the Shanghai observatory catalogue (Wan et al, 1980), and almost all use the maximum likelihood method outlined by Murray (1983). As Table 3 shows, the results show a remarkable consistency, with the most recent analyses agreeing to within 0.15 magnitudes with the mean absolute magnitudes derived at the outset by Strugnell et al (1986), Barnes & Hawley (1986) and Hawley et al (1986).

Layden et al (1996) supplement the Shanghai catalogue with data for field RR Lyraes included in the Lick Northern Proper Motion sample, almost doubling the number of metal-poor stars in the sample. Their analysis also has the benefit of improved radial velocity determinations for many stars. Using Monte Carlo simulations to test the robustness of their solution, they find no suggestion of systematic bias due to inherent sample properties.

Fernley et al (1998) and Tsujimoto et al (1998) have undertaken similar analyses based on Hipparcos data. While the proper motions are typically a factor of two more accurate than in the ground-based catalogue, there is no evidence for any systematic differences. Thus, the derived mean absolute magnitudes are little changed. Gould and Popowski (1998) have also examined critically the photometry, radial velocities and reddening determinations, and find no indication of potential systematic biases in $\langle M_V \rangle$. Similar results follow if they constrain the kinematics using data for spectroscopically-selected field halo stars from Beers & Sommer-Larsen (1995). In summary, statistical parallax analysis of field RR Lyraes consistently leads to faint absolute magnitudes, and provides no empirical evidence for the trend in $\langle M_V \rangle$ with [Fe/H] which is predicted theoretically and derived empirically by other analysis methods, as discussed in the following sections.

Theoretical analyses

Luminosities for both RR Lyraes and non-variable HB stars can be estimated directly from theoretical evolutionary models. Building on the fundamental calculations by Sweigart & Gross (1976), extensive grids of 'standard' models (solar CNO/Fe, no core rotation) were computed by Lee & Demarque (1990 - LD90) and Castellani et al (1991 - CCP), while Dorman (1992) extended calculations to include enhanced CNO abundances. In broad terms, the location of a zero-age horizontal branch (ZAHB) star depends on the mass of the helium core, M_C ($\approx 0.50 M_\odot$ for globulars); the mass of the residual envelope, which is predominantly hydrogen, but with a helium fraction enriched through dredge-up to 0.01-0.02 above Y_{MS}; and the metallicity. Increasing M_C leads to higher luminosities, while the effective temperature is highest (and log L lowest) at the minimum envelope mass: that is, BHB stars are lower mass than RHB stars at given abundance, Z.

Increasing Z for a given total mass leads to lower temperatures, with the effect becoming more pronounced with increasing envelope mass. Hence, while the LD90 models predict only a modest change in the effective temperature range spanned by [Fe/H]=-2.25 and -1.25 ZAHB models ($4.4 > logT_{eff} > 3.75$ versus $4.32 > logT_{eff} > 3.72$), the mass distribution is markedly less uniform, with the higher mass stars concentrated at low temperatures. This is the first-order explanation for the change in HB morphology with abundance, and there are three important consequences for the expected properties of RR Lyrae stars. First, Bono & Stellingwerf (1994) have shown that the location of the instability strip is relatively insensitive to abundance, with (to within $\sim$ 150K) overtone pulsation stable for $7200 > T_{eff} > 6500$K and fundamental pulsation viable over the range $6900 > T_{eff} > 5900$.[6] Combined with evolutionary models, the prediction is that RR Lyraes in intermediate-abundance clusters (such as M5) are lower-mass than their counterparts in metal-poor systems. In particular, the LD90 models predict 0.65-0.70 $M_\odot$ and 0.75-0.90 $M_\odot$ respectively.

These predictions can be tested using data for RRd variables in globulars. analysing double-mode Cepheids, Petersen (1973) demonstrated that, since the pulsation constants depend only weakly on luminosity, T_{eff} and composition, the overtone/fundamental period ratio, P_1/P_0, is determined primarily by the mass and radius (or $\langle\rho\rangle$). Hence, stars of a given mass occupy a narrow locus in the (P_1/P_0, P_0) plane - the Petersen diagram. The same technique can be applied to RRd stars, and initial results indicated masses $\sim 0.1M_\odot$ lower than the evolutionary predictions: $\sim 0.55M_\odot$ at [Fe/H]~ -1.3 (M3) and $\sim 0.65M_\odot$ at [Fe/H]~ -2.1 (M15). However, both Kovacs et al (1991) and Cox (1991) showed that adopting Iglesias and Rogers' (1992) opacities, rather than the Los Alamos calculations used previously, led to increases of $\sim 0.1M_\odot$ in the mass derived from linear pulsational analysis. Full nonlinear calculations by Bono et al (1996) give even higher mass estimates, with $\sim 0.70M_\odot$ for M3 variables and $\sim 0.82M_\odot$ for M15 and M68 stars. These results are therefore in good agreement with direct evolutionary calculations.

The second consequence is that as RR Lyrae stars evolve, the predominant direction of evolution is expected to be a function of abundance. In M5-like systems, the majority of variables should evolve from low to high temperature, while the reverse holds for M15-like systems. Recent observations of variable star period-changes (Silbermann & Smith, 1995; Reid, 1996b) tend to support this hypothesis. In particular, Clement et al (1997) have shown that the M3 star V79 has evolved from a fundamental pulsator to a mixed-mode RRd variable, while the strength of the overtone pulsations in V68, an RRD star, have increased. Both results imply blueward evolution. In contrast, there is evidence for more dominant fundamental-mode oscillations in the M15 RRd variable V30, implying redward evolution.

The third consequence concerns the average luminosity of RR Lyraes, which is expected to exceed the level of the ZAHB. In most clusters the offset is ~ 0.1 magnitudes, but Lee et al (1990) emphasise that in clusters with an extremely blue horizontal branch, those stars which reach the instability strip have evolved significantly, can be brighter than M_V(ZAHB) by ~ 0.3 magnitudes. This is only a serious consideration for clusters where Lee's HB-type parameter exceeds 0.9 (M13, NGC 6397, etc).

Quantitative predictions of the luminosity of the ZAHB have been influenced significantly by the inclusion of the revised OPAL opacities (Iglesias & Rogers, 1996) and equation of state (Rogers et al, 1996). Mazzitelli et al (1995) demonstrated that the revised physical parameters predict an increase over the LD90 and CCP models of 0.01 to 0.015 $M_\odot$ in the core mass at the tip of the red giant branch. Cassisi et al (1998) further extend the analysis by including revised

[6]Note the overlap in temperature, considered further in discussion of the Oosterhoff dichotomy.

He-burning (α) rates and updated neutrino energy-loss calculations. They derive slightly higher core masses than even MDC, and HB lifetimes $\sim$ 23% shorter than the CCP models ($\approx$ 80 Myrs vs. 100 Myrs). The latter result has important repercussions, beyond the scope of the current article, for estimating Y_{MS}. Including the effects of helium diffusion, luminosities on the ZAHB at log T_{eff}=3.85 (i.e. the center of the instability strip) are predicted as log(L)=1.68 at [M/H]=-1.3 and log(L)=1.74 at [M/H]=-2.0. Given bolometric corrections of 0.03 mag. (Flower, 1996) and $M_{bol}(\odot)$=4.70 (see above), these imply M_V(ZAHB)=0.53 and 0.38 mag., with $\langle M_V(RR)\rangle$ brighter by up to 0.1 magnitude.

The higher HB luminosities predicted by these most recent models are also in accord with earlier spectroscopic analysis of BHB stars. Stellar atmosphere models can be used to match spectral line profiles to derive (T_{eff}, log(g)) and, given a distance estimate, the mass. The average mass derived in previous studies of metal-poor clusters (M15: Moehler et al, 1995; NGC 6397: de Boer et al, 1995) is no more than 0.5 $M_\odot$, significantly below theoretical expectations. However, this discrepancy is mitigated substantially if one adopts the longer distance scale implied by either the Hipparcos MS-fitting, the OPAL-based ZAHB calibration (Heber et al, 1997), the brighter absolute magnitudes advocated by Walker (1992), Sandage (1993b) and McNamara (1997), and the models calculated by Caloi, D'Antona & Mazzitelli (1997) and Cassisi et al (1998).

Baade-Wesselink and pulsational analyses

Early studies, based primarily on BV photometry, derived inconsistent results, largely because shocks in the RR Lyrae atmospheres (higher density than Cepheids) invalidate the assumption of equal surface brightness at equal color. Later analyses center on longer wavelength colors, notably (V-I) and (V-K), which are less susceptible to these effects, and use more sophisticated model atmospheres. Even so, most are limited to well-behaved phases of the light-curve. Fernley et al (1989) have also combined this technique with the infrared flux method, directly determining m_{bol} at all phases.

Results from field star studies are summarised by Cacciari et al (1992), Skillen et al (1993) and McNamara (1997). Direct analyses of cluster variables (e.g. Cohen, 1992; Storm et al, 1994) give results consistent with the field star data, but with typical uncertainties of $\pm$0.15 to 0.2 magnitudes. Skillen et al's final calibration, based on combined infrared flux/Baade-Wesselink analysis of 29 stars, gives a mean relation of

$$\langle M_V\rangle = (0.21 \pm 0.05)[Fe/H] + (1.04 \pm 0.10) \quad (8)$$

However, McNamara has re-analysed these same stars using more recent Kurucz model atmospheres, and finds a systematic offset of 200-300K between temperatures derived from optical photometry (including (V-I) and (V-R)) and from (V-K) data. Adopting the optical scale, McNamara derives a steeper, more luminous calibration,

$$\langle M_V\rangle = (0.29 \pm 0.05)[Fe/H] + (0.98 \pm 0.04) \quad (9)$$

Further systematic uncertainties remain in analysing the spectroscopic data. The observed radial velocity is an integration over the stellar disk, and therefore underestimates the true pulsational velocity by a factor, p. Fernley (1994) argues that that factor is underestimated in standard analyses; hence the change in radius, linearly dependent on p, is also underestimated; and the zeropoint should be brighter by 0.07 magnitudes. Adjusting McNamara's relation, this implies $\langle M_V \rangle = 0.58 \pm 0.1$ for M5 variables and 0.29 ± 0.1 in M15. On the other hand, Bono et al (1994) point out that velocity gradients and changes in the opacity within the atmosphere during the pulsational cycle can lead to cross-correlation techniques *overestimating* the true velocity.

Another absolute-magnitude calibration method tied to the pulsational characteristics of RR Lyraes is Fourier decomposition of the light curves. Simon & Clement (1993) have applied this technique to RRc variables, concentrating on the Fourier term, ϕ_{31}. Matched against hydrodynamic models, their results indicate a steep gradient and bright zeropoint, $M_V \approx 0.36[Fe/H] + 0.96$, close to McNamara's recent Baade-Wesselink results. In contrast, Kovacs & Jurcsik (1996) use similar techniques to analyse RRab cluster variables, deriving $M_V \approx 0.19[Fe/H] + 1.04$.

Period shifts and the Oosterhoff dichotomy

Following Bailey's discovery of the first cluster variables, globular clusters became the targets of many photographic studies during the early 20th century. Collecting the results from those studies, Oosterhoff(1939, 1944) computed the mean period for the RRab-types in each cluster, and identified an apparent bimodality in that distribution, with peaks at $\langle P_{ab} \rangle \sim 0^d.55$ (type I) and $0^d.65$ (type II). Arp (1955) first noted that the division between type I and II was also a division by abundance, with type II systems limited to the most metal-poor clusters, such as M15 and M30. Finally, in a detailed study of the RR Lyraes in several clusters, notably M3 and M15, the archetypical type I and II clusters, Sandage (1981) presented evidence for both systematic cluster-to-cluster offsets in the mean period-amplitude and period-temperature (but not amplitude-temperature) relation, and star-to-star offsets at fixed temperature. Interpreting and understanding these observational results is crucial to determining the RR Lyrae (M_V/[Fe/H]) relation.

Most interpretations of these effects are based on the pulsation equation for RR Lyraes. The fundamental equation, $P\sqrt{\langle \rho \rangle} = Q$, where P is the period, ρ the density and Q the pulsation constant, holds for homologous systems. Substituting for ρ allows one to write this equation in terms of mass, luminosity and effective temperature. In the case of RR Lyraes, as with all stars, differences in chemical composition mean that the stars are not homologous, but van Albada & Baker (1971), from analysis of stellar models, showed that a very similar relation holds

$$logP_{ab} = -0.34M_{bol} - 0.68log\frac{M}{M_\odot} - 3.48logT_{eff} + const. \qquad (10)$$

Kovacs et al (1991: see also Fernley, 1993) repeat this analysis, using models based on the revised Livermore opacities (Rogers & Iglesias, 1992), and find that these coefficients vary by up to $\approx 10\%$ over the abundance range spanned by the Galactic halo. Irrespective of those variations, this equation indicates that a difference in period at the same effective temperature implies either a difference in mass, or a difference in luminosity.

In qualitative terms, the Oosterhoff dichotomy is generally agreed to result from the change in morphology of the horizontal branch with decreasing abundance in old (> 10 Gyr) stellar systems (Catelan, 1992; Sandage 1993a and refs within). In metal-rich clusters, such as 47 Tuc, the horizontal branch lies redward of the instability strip, and there are no 'traditional' RR Lyraes. Decreasing abundance leads to a migration to higher temperatures, until, at abundances of between ~ -1.7 and -1.9 dex, the horizontal branch lies blueward of the instability strip. At lower abundances, the trend reverses, and the instability strip is well populated in clusters such as M15 and M68, although less so in M92. The physical origin of the Oosterhoff phenomenon, however, remains a subject of debate, with two main explanations proposed: evolutionary hysteresis and an increased luminosity with decreasing abundance.

van Albada & Baker (1973) originated the hysteresis hypothesis. As discussed above, evolutionary models predict (and observations tend to confirm) that metal-poor RR Lyraes originate from the blue HB and evolve from high to low temperatures, while the opposite holds for intermediate abundance systems. Hence Oo I HB stars evolve initially from long-period to short-period as RRab variables before becoming higher-temperature RRc-types. In contrast, type II variables evolve from RRc-type to fundamental-mode pulsators. van Albada and Baker proposed the existence of an 'either-or' temperature zone, where both fundamental and first overtone pulsations were stable. Under this scenario, Oo II variables switch to fundamental pulsation at a lower temperature than their type I counterparts, leading to a longer average period $\bar{P}_{ab}$ and a higher fraction of c-type stars in metal-poor systems.

The alternative model (Sandage, 1958, 1982) is that HB luminosity (hence $\bar{P}_{ab}$) increases as [M/H] decreases. analysing both cluster data and Lub's (1987) observations of field stars, Sandage (1993a) argues that this is a continuous relation, and that the apparent dichotomy amongst cluster variables arises solely from the change in HB morphology with [M/H]. A similar trend is evident amongst RRc cluster variables, although Simon & Clement (1993) identify temperature differences as the likely source of $\delta\langle P_c\rangle$ between M5 and M68. Sandage, however, also finds systematic differences in period when comparing *individual* stars at the same temperature in clusters of different abundances. The last is the Sandage period-shift effect (SPSE). Given a gradient of $\frac{\partial log(P_{ab})}{\partial [Fe/H]} = -0.12$ for stars at the blue fundamental edge (BFE), combined with abundance-dependent relations for mass, T_{eff}(BFE) ($\frac{\partial T}{\partial [Fe/H]} = 0.012$) and bolometric correction, Sandage (1993b) deduces a mean relation for the horizontal branch of $\langle M_v\rangle \propto 0.30[Fe/H]$.

Both hysteresis and luminosity variation likely play a role in the Oosterhoff dichotomy. As noted above, Bono et al (1995) predict that the fundamental and overtone pulsation zones overlap in temperature, while RRc variables are more than twice as common in type II than type I clusters (45% vs 20%). Hysteresis, however, cannot account for the SPSE. Lee et al's (1990) proposed explanation of higher luminosities due to evolution above the ZAHB is not viable in Oo II clusters with both BHB and RHB stars (M15, M68). Caputo & de Santis (1992) have challenged both the cluster reddenings adopted by Sandage and his temperature scale for RRab variables. Catelan (1992), however, has shown that uncertainties in the former are insufficient to account fully for the

SPSE, while Fernley (1993) finds excellent agreement between the latter scale and his (V-K)-based temperature calibration.

Catelan and Fernley both derive shallower gradients than Sandage's period-abundance relation, $\frac{\partial P}{\partial [Fe/H]} \sim -0.06$ to -0.09. However, a shallower period-shift relation does not necessarily imply a shallower gradient $\frac{\partial \langle M_V \rangle}{\partial [Fe/H]}$ Fernley uses his near-infrared SPSE analysis and the theoretical pulsation relations to derive

$$\langle M_V \rangle \quad = \quad 0.19[Fe/H] \quad + \quad 0.84 \tag{11}$$

That analysis, however, is based on a value of $M_{bol}(\odot)$=4.75 and assumes little variation in mass between Oo I and Oo II RR Lyraes. If one adopts the most recent RRd mass calibration (0.65 and 0.80 $M_\odot$ respectively) and $M_{bol}(\odot)$=4.70, then Fernley's near-infrared data imply $\langle M_V(RRab) \rangle \sim 0.45$ for M15 and ~ 0.8 for M5 i.e. $\langle M_V \rangle \propto 0.35$[Fe/H].

Main-sequence fitting calibration of cluster variables

The RR Lyrae ($\langle M_V \rangle$, [Fe/H]) relation can be estimated directly from globular cluster color-magnitude diagrams given a distance scale calibration, such as the Hipparcos-based results tabulated in the previous section. The main limitation rests with the availability of high-accuracy CCD photometry, since most studies concentrate on low-luminosity main-sequence stars, rather than evolved stars. Time-resolved data are particularly sparse. To date, the clusters with sufficient observations to defined $\langle V_0(RRab) \rangle$ are the Oo I cluster M5 (Reid, 1996b) and the three Oo II clusters M15 (Silbermann & Smith, 1995), M68 (Walker, 1994) and M92 (Carney et al, 1992). The corresponding values of $\langle M_V(RRab) \rangle$, given the distance moduli and reddening listed in the final column of Table 2, are 0.5, 0.32, 0.32 and 0.26 - implying $M_V \propto 0.2[Fe/H]$ and a bright zeropoint.

Summary

The various techniques outlined above can be divided into two categories based on the deduced RR Lyrae absolute magnitude calibration: direct trigonometric parallax and statistical parallax analyses favor $\langle M_V \rangle \sim 0.75 \pm 0.15$, with little or no variation with abundance; other methods favor a steeper (M_V, [Fe/H]) relation and, usually, a brighter zeropoint (figure 6). Deciding between these alternatives is not straightforward. The local RR Lyrae sample is dominated by relatively metal-rich stars ([Fe/H]> -1.4), but a brighter zeropoint in M_V also implies higher velocity dispersions, at odds with other tracers of the halo population. Gould & Popowski (1998) suggest that the problem lies in a mismatch between the cluster and field-subdwarf metallicity scales, with the clusters significantly lower abundance than the CG97 giant-based scale. However, reducing the M15 distance modulus by 0.4 magnitudes to accommodate $\langle M_V \rangle$(RR) ~ 0.8 requires adjusting the (B-V) colors of the field subdwarfs by -0.07 mag., placing those stars well blueward of even the most extreme metal-poor isochrones.

Demanding that the field and cluster calibrations agree assumes that the two sets of variables have identical absolute magnitude distributions. Cluster red giants exhibit abundance anomalies which have yet to be detected in halo giants in the field (Shetrone, 1997). Sweigart (1997) points out that if those anomalies stem from deep mixing, the atmospheric helium content can also be increased, leading to higher luminosities and hotter temperatures on the horizontal branch. Catelan (1998), however, suggests that the good agreement between the period-temperature distributions of field and cluster RR Lyraes argues against significant luminosity differences. Currently, the majority of analysis techniques favor the steep (M_V, [Fe/H]) relation derived originally by Sandage (1982).

6.4. Mira variables

Observations of long-period asymptotic giant-branch variables (Miras) in the Magellanic Clouds have established that, like Cepheids, those stars follow a period-luminosity relation, best-defined in the 2.2μm K-band (Feast et al, 1989). Hipparcos obtained astrometry for 180 Galactic Miras, with the highest-precision measurement having an accuracy of 10.5% (R Car). van Leeuwen et al (1997) follow the precepts outlined by Feast & Catchpole in the latter's Cepheid study in analysing a sub-sample of 16 Miras, pre-selected using parallax-independent criteria. Fixing the slope of the period-luminosity relation using LMC variables, the preferred relation ($(\frac{1}{\sigma_\pi})^2$ solution) is

$$M_K \quad = \quad -3.47 \quad logP \quad + \quad 0.88 \pm 0.18$$

7. The local distance scale

Revised calibrations for distance indicators inevitably lead to revised distance estimates. We summarise those results in the context of other recent analyses, concentrating on Cepheids and horizontal branch stars. More extensive reviews of measurements of R_0 and distance estimates to the Magellanic Clouds are provided by Reid (1993) and Walker (1998) respectively. Given the continuing uncertainties, as far as possible we avoid the temptation to rationalise discrepancies and arrive at preferred values.

7.1. The distance to the Galactic center

Rotation constants: the Solar Radius can be derived from the Oort constants, $A = -\frac{1}{2}R_0(\frac{d\Omega}{dR})_0$ and $B = -\Omega_0 - \frac{1}{2}R_0(\frac{d\Omega}{dR})_0$, where Ω_0 is the local angular rotation velocity, $\frac{\Theta_0}{R_0}$. Feast and Whitelock (1998) combine Hipparcos Cepheid proper-motion data with Pont et al's (1997) radial velocities to derive $\Omega_0 = 27.19 \pm 0.87 \mathrm{kms}^{-1}\mathrm{kpc}^{-1}$ and $R_0 = 8.5 \pm 0.5$ kpc. They derive similar results if they scale Metzger et al's (1998) Cepheid distance scale to match the Hipparcos P-L relation zeropoint; Metzger et al's own determination is 7.66±0.54 kpc.

Feast and Whitelock's analysis implies $\Theta_0 \sim 230 \mathrm{kms}^{-1}$. Olling & Merrifield (1998), however, have modelled the local rotation curve, and find that variations in the surface density lead to non-linear behaviour in the Oort functions, A(R) and B(R). They argue that those variations account for the range of values for A & B derived in studies sampling sources at different heliocentric distances. Their best-fit solution has a significantly lower local velocity of rotation, $\Theta_0 = 184 \pm 8$kms^{-1} and R_0=7.1±0.4 kpc.

Geometric determinations: Proper-motion and radial velocity data for H_2O masers allow the derivation of an expansion parallax. analysis of the Sgr B2 (North) complex, $\approx$ 300 pc. from the Galactic center, leads to a value of $R_0 = 7.1 \pm 1.5$kpc, while averaging several other studies gives $R_0 = 7.2 \pm 0.7$ kpc (Reid, 1993). Alternatively, the measured proper motion of Sgr A* ($\mu_l = -6.55 \pm 0.17$ mas yr^{-1}, $\mu_b = -0.48 \pm 0.06$ mas yr^{-1}; Backer, 1996, interpreted as reflex Solar motion, can be used to constrain $\frac{\Theta_0}{R_0}$. Adopting $V_\odot = 12$ kms^{-1} relative to the Local Standard of Rest, then if $170 < \Theta_0 < 240$ kms^{-1}, R_0 is constrained to lie between 5.9 and 8.1 kiloparsecs.

Red clump stars: The OGLE and MACHO microlensing surveys have fueled extensive studies of the color-magnitude distribution of both the Magellanic Cloud and Bulge stellar populations. Paczyinski and Stanek (1998) derive a mean magnitude for $\langle I_0 \rangle = 14.32$ for red clump stars in the lower-reddening ($A_V < 1.5$) regions of Baade's window. Locally, the red clump star observed by Hipparcos have $\langle M_I \rangle = -0.18$, which Paczynski and Stanek correct to $\langle M_I \rangle = -0.28$. As noted in the previous section, the local clump stars are bluer than their Bulge counterparts ($\langle (V-I)_0 \rangle \sim 1.0$ versus $\langle (V-I)_0 \rangle \sim 1.25$), but if one assumes that the stellar populations are compatible, then this implies a distance modulus of $(m\text{-}M)_0 = 14.60$ magnitudes to the centroid of the Baade's window population. Adjusting that estimate to the Galactic center, Paczynski & Stanek derive $(m\text{-}M)_0$=14.62, or $R_0 = 8.4 \pm 0.4$ kpc.

RR Lyraes: the Galactic bulge variables have an average abundance of [Fe/H]~ -1 (Walker & Terndrup, 1991), comparable with the globular cluster M5. Both cluster and Bulge RR Lyraes describe well-defined relations in the (logP, K) plane, with an offset in zeropoint in the sense that the Bulge stars are fainter (Reid, 1998). If both sets of RR Lyraes have identical absolute magnitude distributions, then a distance modulus of 14.5 to M5 implies $(m\text{-}M)_0$=14.8 to the centroid of the Bulge variables, or $R_0 = 9.1 \pm 0.4$ kiloparsecs.

7.2. The distance to the Large Magellanic Cloud

SN 1987A: The fortuitous existence of a gaseous ring surrounding the progenitor of SN 1987A permits a geometric estimate of its distances. As originally discussed by Panagia et al (1991), the time delay between the onset of fluorescence in forbidden lines of C and N, and the maximum luminosity in those lines (observed by the IUE satellite) provides a a measure of the linear dimensions of the ring, while imaging by HST allows measurement of the angular dimensions. Gould & Uza (1998) employ sophisticated light-curve analysis to determine an upper limit to the distance modulus of $(m\text{-}M)_0 = 18.44$ (for an elliptical ring, $\frac{b}{a} \sim 0.95$). However, Panagia (1998) points out that their analysis omits a crucial factor: the SN 1987A ring is expanding; hence the diameter measured by HST in 1990 overestimates the angular size at maximum fluorescence in 1988. Taking the expansion into account, Panagia derives a distance modulus of 18.57±0.1, or a distance of 51.7±2.3 kiloparsecs.

Cepheids and Miras: Laney & Stobie's (1995) pre-Hipparcos Galactic calibration (scaled to a Hyades modulus of 3.33 magnitudes) gives a true distance modulus of 18.58 to the LMC. In comparison, Feast & Catchpole use their Galactic calibration to estimate $(\text{m-M})_0 = 18.70$. As both Sandage & Tamman (1998) and Feast & Whitelock (1998) emphasise, these estimates depend on both the assumed foreground reddening toward the LMC and metallicity corrections. Madore & Freedman (1991) adopt E_{V-I}=0.10 for LMC Cepheids lacking direct measurement, while Feast & Whitelock argue for $E_{V-I} = 0.075$. This translates to $\delta(m-M)_0 \sim 0.1$ mag. for identical Galactic calibrations. Gieren et al (1998) adopt the same reddening corrections as Feast & Catchpole, and no metallicity corrections (Feast & Catchpole adopt +0.042 mag.), and use their Galactic calibration to derive a shorter distance modulus of $(\text{m-M})_0$=18.46 magnitudes, while scaling Di Benedetto's calibration gives $(\text{m-M})_0$=18.64 (Walker, 1998). Finally, van Leeuwen et al's preferred calibration of the Mira period-luminosity relation leads to an estimate of $(\text{m-M})_0$=18.54 magnitudes. Averaging these three estimates gives $(\text{m-M})_0$=18.57, matching the pre-Hipparcos Cepheid value.

Horizontal branch and red clump stars: Population differences between the Galaxy and the LMC complicate the use of these stars, particularly the red clump. The LMC clusters with the highest RR Lyrae frequency (such as NGC 1466) have abundances of [Fe/H]~ -1.8, at which abundance the horizontal branch lies exclusively blueward of the instability strip in the (older) Galactic clusters. Theoretical models predict relatively small luminosity differences, but one must assume that a similar (M_V, [Fe/H]) relation holds for both systems. Given $\langle V_0 \rangle = 18.98$ for the LMC cluster variables (Walker, 1994), the Galactic RR Lyrae statistical parallax calibration ($M_V = 0.77 \pm 0.15$) implies $(\text{m-M})_0 \sim 18.2$, compatible with the value derived from red clump stars (Udalski et al, 1998). On the other hand, the steeper (M_V, [Fe/H]) relation favored by the preponderance of Galactic cluster calibrations implies $\langle M_V \rangle \sim 0.35$ to 0.4 at [Fe/H]=-1.8, and an LMC modulus of $(\text{m-M})_0 \sim 18.60$. The latter is in better accord with estimates based on other distance indicators, notably SN1987A.

7.3. Distances to the SMC and M31

The SMC

The relative distance modulus between the LMC and the SMC can be determined through observations of both Cepheids and RR Lyraes, making due allowance for the significant depth of the latter system over much of its area. RR Lyraes in NGC 121 ([Fe/H]~ -1.9) have $\langle V_0 \rangle = 19.46 \pm 0.07$ (Walker & Mack, 1988), implying $\delta(\text{m-M})_0 = 0.48 \pm 0.07$ relative to the average of the LMC clusters. Udalski's (1998) analysis of field RR Lyraes leads to a slightly higher relative distance, δ(m-M)$_0$ = 0.52 ± 0.05, although reddening and possible abundance differences are a complication in this comparison. analyses of LMC and SMC Cepheids (Laney & Stobie, 1995; di Benedetto, 1997), on the other hand, favor δ(m-M)$_0$ = 0.42 ± 0.04. Thus, the available estimates span a only limited range.

M31

Distance estimates for M31 are based primarily on observations of fundamental distance indicators, with the high spatial resolution provided by HST rendering globular cluster HB stars accessible. As with the SMC, direct determinations based on Galactic calibrations can be complemented by measuring the relative distance modulus with respect to the LMC.

Cepheids: Freedman & Madore (1990) derive a relative distance modulus of $\langle \delta(m-M)_0^{M31-LMC} \rangle = 5.89$mag. using observations of variables in Baade's fields I, III and IV, while Kochanek (1997) derives $5.8 < \delta(m-M)_0 < 5.97$ for a range of metallicity relations. One should note, however, that Freedman & Madore derive $\delta(m-M)_0 = 6.10$mag. from data for ~ 50 Cepheids in Baade's field IV, the outermost field, which has both negligible foreground reddening and a metallicity ($\frac{Z}{Z_\odot} \sim 0.3$) close to that of the LMC. Comparative results for RR Lyraes are also consistent with a longer modulus.

RR Lyraes: Pritchet & Van den Bergh (1987) obtained the first photometry of RR Lyraes in the halo of M31, deriving $\langle B \rangle = 25.68 \pm 0.06$. Fusi-Pecci et al (1996) and Holland et al (1997) have taken advantage of HST to determine color-magnitude diagrams for ten M31 globulars ranging from [Fe/H]=-0.2 to -2.3 dex. Assuming a linear relation, $V_0(HB) = \alpha[Fe/H] + \beta$, a least-squares fit to the mean HB magnitudes gives $\alpha = 0.13 \pm 0.07$, $\beta = 25.38 \pm 0.09$, slightly shallower than deduced for Galactic cluster variables. Considering individual clusters, the three lowest-abundance systems are G219 ([Fe/H]=-2.28), G351 (-1.95) and G302 (-1.85), with V_0(HB) = 25.10, 25.16 and respectively. Adopting V_0(HB)=25.13 at [Fe/H]=-2.1 gives $\delta(m-M)_0^{M31-LMC} = 6.15$ to 6.25 for $0 < \alpha < 0.35$, or (m-M)$_0^{M31}$ = 24.75 to 24.85 for (m-M)$_0^{LMC}$ = 18.6. Direct comparison with data for the Galactic clusters M68 and M15 gives $\delta(m-M)_0^{M31-M68} = 9.70$ ((m-M)$_0^{M31}$ = 24.81 if the M68 modulus is taken from the final column of Table 2) and $\delta(m-M)_0^{M31-M15} = 9.59$ ((m-M)$_0^{M31}$ = 24.82) respectively. Similarly, one can average Fusi Pecci et al's result for G1 ([Fe/H]=-1.33, V_0(HB)=25.15) and G105 (-1.25, 25.30) to estimate V_0(HB)=25.22 at [Fe/H]=-1.3. Matching against M5 gives a relative distance modulus of 10.22 to 10.29 ($0 < \alpha < 0.35$) and (m-M)$_0^{M31}$ = 24.72 to 24.79, consistent to within 0.1 magnitude with the estimates based on the metal-poor RR Lyraes.

Red clump stars: Stanek & Garnavich (1998) have used HST observations to measure $\langle I_0 \rangle = 24.27$ for red clump stars in three fields in M31. Coupled with their Hipparcos-based Galactic calibration, they derive (m-M)$_0$ = 24.47 ± 0.05, a value identical with Freedman & Madore's (1990) result. However, the latter value is based on (m-M)$_0^{LMC}$ = 18.50 and $\delta(m-M)_0^{M31-LMC} = 5.89$mag., while Udalski et al (1998) derive $\langle I_0 \rangle = 17.85$ for LMC red clump stars, giving $\delta(m-M)_0^{M31-LMC} = 6.42$mag and (m-M)$_0^{LMC}$ = 18.04. These inconsistencies underline current uncertainties in using red clump stars as distance indicators.

8. Conclusions and prognosis

From the preceding discussion it should be clear that the Hipparcos results do not, in and of themselves, provide definitive resolution of any of the major questions associated with the determination of the Galactic distance scale. This is not surprising, since the main achievement lies in extending greatly the sample of stars with accurate astrometry, rather than pushing that accuracy beyond the best ground-based limits. Nonetheless, these data have catalysed a general reappraisal of several issues of fundamental importance and have underlined the potential of space-based astrometry. Several satellite missions are under consideration for launch over the next decade to capitalise on this potential.

Among the acronym-rich proposed future projects are DIVA, GAIA and SIM. DIVA (Röser et al, 1997) is proposed for launch as early as 2002, and marks an extension of the Hipparcos project, with twin-beamed Fizeau interferometers used to determine positions to 0.5 mas for all stars with V$<$ 10.5 and a limited sample extending to 15th magnitude. GAIA (Lindegren & Perryman, 1996) is an interferometric satellite observatory, proposed for ESA's Horizon 2000+ plan. The aims include observations of astronomical targets to 16th visual magnitude, including all sources brighter than 15th magnitude (a total of 50 million objects), with an accuracy of 10μarcsec at V=15.

Finally, and most ambitiously, the Space Interferometry Mission (SIM), a 5- to 10-year mission scheduled for launch in 2006, aims to achieve a precision of 1 μarcsec in relative measurements over small ($< 5^o$) angles, and an overall accuracy of 4 μarcsec in absolute astrometry. The latter capability will permit trigonometric parallax measurements of not only all primary distance-scale calibrators, but also direct distance determinations for stars in the nearer globular clusters. If achieved, those observations should finally settle the remaining discrepancies in at least the local distance scale.

Bob Hanson provided helpful comments and insight on systematic problems associated with parallax measurements.

REFERENCES

Allard F, Hauschildt PH, Alexander DR, Starrfield S 1997. ARA&A35:137-177

Alonso A, Arribas S, Martínez-Roger C 1996. A&AS117:227-254

Arenou F, Lindegren L, Froeschle M, Gómez AE, Turon C, Perryman MAC, Wielen R 1995. A&A304:52-60

Arp HC 1955. AJ60:317-337

Axer M, Fuhrmann K, Gehren, T 1994. A&A291:895-909

Baade, W 1926. Astr Nacht 228:359-362

Backer DC 1996. in *IAU Symposium 169*, eds L. Blitz & P. Teuben, (Reidel: Dordrecht, Netherlands), pp 23-29

Barnes TG, Evans DS 1976. MNRAS174:489-502

Barnes TG, Hawley SL 1986. ApJ307:L9-L13

Beaulieu JP, Sackett PD 1998. AJ116:209-219

Beers TC, Sommer-Larsen J 1995. ApJS96:175-221

Bergbusch P, Vandenberg DA 1992. ApJS81:163-220

Bertelli G, Bressan A, Chiosi C, Fagotto F, Nasi E 1994 A&AS106, 275-302

Biémont E, Baudoux M, Kurucz RL, Ansbacher W, Pinnington EH 1991. A&A, 249:539-544

de Boer KS, Schmidt JHK, Heber U 1995. A&A303:95-106

de Boer KS, Tucholke HJ, Schmidt JHK 1997. A&A317:L23-L26

Bolte M 1992. ApJS82:145-165

Bolte M, Hogan CJ 1995. Nature 376:399-402

Bono G, Caputo F, Stellingwerf RF 1994. ApJ432:L51-L54

Bono G, Caputo F, Marconi M 1995. AJ110:2365-2368

Bono G, Caputo F, Castellani V, Marconi M 1996. ApJ471:L33-L36

Bono G, Stellingwerf RF 1994. ApJS93:233-269

Burstein D, Heiles C 1982. AJ87:1165-1189

Cacciari C, Clementini G, Fernley JA 1992. ApJ396:219

Caloi V, D'Antona F, Mazzitelli I 1997. A&A320:823-830

Caputo F, De Santis R 1992. AJ104:253-261

Carney BW, Latham DW, Laird JB, Aguilar LA 1994. AJ107:2240-2289

Carney BW, Storm J, Trammell SR, Jones RV 1992. PASP104:44-56

Carretta E, Gratton RG 1997. A&AS121:95-112

Cassisi S, Castellani V, Degl'Innocenti S, Weiss A 1998. A&AS129:267-279

Castellani V, Chieffi A, Pulone L 1991. ApJS76:911-977

Catelan M 1992. A&A261:457-471

Catelan M 1998. ApJ495:L81-L84

Cayrel de Strobel G, Soubiran C, Friel ED, Ralite N, Francois P 1997. A&AS124:299-305

Cayrel R, Lebreton Y, Perrin M-N, Turon, C 1997. in *Hipparcos Venice '97*, ed B Battrick (ESA), pp 219-223

Chaboyer B, Demarque P, Kernan PJ, Krauss LM 1996. Science 271:957-961

Chaboyer B, Demarque P, Kernan PJ, Krauss LM 1998. ApJ494:96-110

Chiosi C, Wood PR, Capitanio N 1993. ApJS86:541-598

Clement CM, Hilditch RW, Kaluzny J, Rucinski SM 1997. ApJ480:L55-L58

Clementini G, Gratton RG, Carretta E, Sneden C 1999. MNRAS302:22-36

Cohen JG 1983. ApJ270:654-665

Cohen JG 1992. ApJ400:528-534

Cole AA 1998. ApJ500:L137-L140

Cool AM, Piotto G, King IR 1996. ApJ468:655-662

Cox AN 1991. ApJ381:L71-L74

D'Antona F, Caloi V, Mazzitelli I 1997. ApJ477:519-534

Detweiler HL, Yoss KM, Radick RR, Becker SA 1984. AJ89:1038-1038

Di Benedetto GP 1997. ApJ486:60-74

Dorman B 1992. ApJS81:221-250

Eggleton PP, Faulkner J, Flannery BP 1973. A&A23:325-330

ESA 1997. The Hipparcos and Tycho Catalogues, ESA SP-1200 (Noordwijk: ESA)

Feast MW, Walker AR 1987. ARA&A25:345-375

Feast MW, Glass IS, Whitelock PA, Catchpole RM 1989. MNRAS241:375-392

Feast MW, Catchpole, RM 1997. MNRAS286:L1-L5

Feast MW, Whitelock, PA 1998. MNRAS291:683-693

Feast MW, Pont F, Whitelock P 1998. MNRAS298:L43-L44

Feast MW 2000. PASP, in press

Fernandes J, Lebreton Y, Baglin A 1996. A&A311:127-134

Fernley J 1993. A&A268:591-606

Fernley J 1994. A&A284:L16-L18

Fernley JA, Lynas-Grey AE, Skillen I, Jameson RF, Marang F, Kilkenny D, Longmore AJ 1989. MNRAS236:447-473

Fernley JA, Barnes TG, Skillen I, Hawley SL, Hanley CJ, Evans DW, Solano E, Garrido R 1998. A&A330:515-520

Flower PJ 1996. ApJ469:355-365

Flynn C, Morell O 1997. MNRAS286:617-625

Fouqué P, Gieren WP 1997. A&A320:799-810

Freedman WF, Madore BF 1990. ApJ365:186-194

Fusi Pecci F, Buonnanno R, Cacciari C, Corsi CE et al 1996. AJ112:1461-1471

Gatewood G, De Jonge JK, Persinger T 1998. AJ116:1501-1503

Gieren WP, Mermilliod J-C, Matthews JM, Welch DL 1996. AJ111:2059-2065

Gieren WP, Fouqué P, Gómez M 1997. ApJ, 488:74-88

Gieren WP, Fouqué P, Gómez M 1998. ApJ, 496:17-30

Girardi L, Groenewegen MAT, Weiss A, Salaris M 1998. MNRAS, 301:149-160

Gizis JE 1997. AJ113:806-822

Gould A, Popowski P 1998. ApJ508, 844-853

Gould A, Uza O 1998. ApJ494:118-124

Gratton RG 1998. MNRAS296:739-745

Gratton RG, Carretta E, Castelli F 1997a. A&A314:191-203

Gratton RG, Fusi Pecci F, Carretta E, Clementini G, Corsi CE, Lattanzi M 1997b. ApJ491:749-771

Gustafsson B, Bell RA 1979. A&A74:313-352

Hanson RB 1979. MNRAS186:875-896

Harris HC,Dahn CC, Monet D 1997. in *Hipparcos Venice '97*, ed B Battrick (ESA), pp. 105-110

Harris WE 1996 AJ112:1487-1488

Hawley SL, Jeffreys WH, Barnes TG, Wan L 1986. ApJ302:626-631

Heber U, Moehler S, Reid IN 1997. in *Hipparcos Venice '97*, ed B Battrick (ESA), pp. 461-464

Holland, S, Fahlman GG, Richer HB 1997. AJ114:1488-1507

Huebner WF, Merts AL, Magee NH, Argo MF 1977. Los Alamos Sci Lab Rept (LA-6760-M)

Iglesias CA, Rogers FJ 1992. ApJ443:460-463

Iglesias CA, Rogers FJ 1996. ApJ464:943-953

Jahreiss H, Gliese W 1991. Preliminary version of the third Nearby Star Catalogue

Jimenez R, Flynn, C Kotoneva, E 1998. MNRAS219:515-519

Jones JB, Gilmore GF, Wyse RFG 1996. MNRAS278:146-182

King IR, Anderson J, Cool AM, Piotto G 1998. ApJ492:L37-L40

King JR 1997. AJ113:2302-2311

King JR, Stephens A, Boesgaard AM, Deliyannis CP 1998. AJ115:666-684

Kochanek CS 1997. ApJ491:13-28

Koen C 1992. MNRAS256:65-68

Kovacs G, Buchler JR, Marom A 1991. A&A252:L27-L30

Kovacs G, Jurcsik J 1996. ApJ466:L17-L20

Kovalevsky J 1998. ARA&A36:99-129

Kraft RP 1961. ApJ134:616-632

Kraft RP, Sneden C, Langer GE, Shetrone MD 1993. AJ106:1490-1507

Kurucz RL 1992 in *The Stellar Populations of Galaxies*, IAU NSymposium 149, eds B Barbuy & A. Renzini, (Luwer: Dordrecht), pp 225-228

Laney CD, Stobie RS 1994. MNRAS266:441-454

Laney CD, Stobie RS 1995. in *Astrophysical Applications of Stellar Pulsation*, eds RS Stobie, & PA Whitelock, ASP Conf Ser 83. 254-258

Layden AC, Hanson RB, Hawley SL, Klemola AR, Hanley CJ 1996. AJ112:2110-2131

Lee Y-W, Demarque P 1990. ApJS73:709-746

Lee Y-W, Demarque P, Zinn R 1990. ApJ350:155-172

Lindegren L, 1988. in *Scientific Aspects of the Input Catalogue Preparation II*, Proc. Colloq. Sitges (Catalonia), eds J. Torra & C. Turon, p. 179-185

Lindegren L, 1995. A&A304:61-68

Lindegren L, Perryman MAC 1996. A&AS116:579-595

Lindegren L, Röser S, Schrijver H, Lattanzi MG, van Leeuwen F, Perryman MAC, Bernacca PL, Falin JL, Froeschle M, Kovalevsky J, Lenhardt H, Mignard F 1995. A&A304:44-51

Lub J 1987. in *Stellar pulsations*, (Springer-Verlag: New York & Berlin), pp 218-229

Lutz TE, Kelker DH 1973. PASP85:573-578

Lutz TE, 1983. in *IAU Coll. 76: The Neraby Stars and the Stellar Luminosity Function*, eds AGD Phillips & AR Upgren, L Davis Press, Schenectady, 41-50

Lynga G, Lindegren L 1998. New Astr 3:121-123

McNamara DH 1997. PASP109:857-867

McWilliam A, Rich RM 1994. ApJS91:749-791

Madore BF, Freedman WL 1991 PASP103:933-957

Madore BF, Freedman WL 1998 ApJ492:110-115

Mazzitelli I, DAntona F, Caloi V, 1995. A&A302:382-400

Mermilliod J-C, Robichon N, Arenou F, Lebreton Y 1997. in *Hipparcos Venice '97*, ed B Battrick (ESA), 643-650

Metzger MR, Caldwell JA, Schechter PL 1998. AJ115:635-647

Moehler S, Heber U, de Boer KS 1995. A&A294:65-79

Monet DG 1988. ARA&A26:413-440

Murray CA 1983. Vectorial astrometry, p 297. Adam Hilger, Bristol

Nissen PE, Hog E, Schuster WJ 1997. in *Hipparcos Venice '97*, ed B Battrick (ESA), pp 225-230

Olling RP, Merrifield MR 1998. MNRAS297:943-952

Oosterhoff P 1939. Observatory 62:104-109

Oosterhoff P 1944. Bull Astr Inst Netherlands 10:55-58

Oudmaijer RD, Groenewegen MAT, Schrijver H 1997. MNRAS294:L41-L46

Paczyński B 1998. Acta Astr 48:405-412

Paczyński B, Stanek K 1998. ApJ494:L219-L222

Pagel BEJ, Portinari L 1998. MNRAS298:747-752

Panagia N, Gilmozzi R, Machetto F, Adorf HM, Kirshner RP 1991. ApJ380:L23-L26

Panagia N 1998. Mem. Soc. Astron. Ital. 69:225-235

Perryman MAC, Brown AGA, Lebreton Y, Gómez A, Turon C, Cayrel de Strobel G, Mermilliod J-C, Robichon N, Kovalevsky J, Crifo F 1998. A&A331:81-120

Petersen JO 1973. A&A27:89-93

Peterson RC, Kurucz RL Carney BW 1990 ApJ350:173-185

Pinsonneault MH, Stauffer J, Soderblom DR, King JR, Hanson RB 1998. ApJ504:170-191

Pont F, Queloz D, Bratschi P, Mayor M 1997. A&A318:416-428

Pont F, Mayor M, Turon C, Vandenberg DA 1998. A&A329:87-100

Pritchet CJ, van den Bergh S 1987. ApJ316:517-529

Rees RF 1997. in *Proper Motions and Galactic Astronomy*. ASP Conf. ser. vol. 127, ed. RM Humphreys, pp 109-115

Reid IN, Murray CA 1992. AJ103:514-528

Reid IN 1996a AJ111:2000-2016

Reid IN 1996b MNRAS278:367-394

Reid IN 1997. AJ114:161-180

Reid IN 1998. AJ115:204-228

Reid IN, Gizis JE 1998. AJ116:2929-2935

Reid MJ 1993. ARA&A31:345-372

Renzini A, Bragaglia A, Ferraro FR, Gilmozzi R, Ortolani S et al 1996. ApJ465:L23-L26

Richer HB, Fahlman GG 1986. ApJ304:273-283

Richer HB, Fahlmann GG, Ibata RA, Pryor C, Bell RA et al 1997. ApJ484:741-760

Robichon N, Arenou F, Turon C, Mermilliod J-C, Lebreton Y 1997. in *Hipparcos Venice '97*, ed B Battrick (ESA), 567-570

Rogers FJ, Iglesias CA 1992. ApJS79:507-568

Rogers FJ, Swenson FJ, Iglesias CA 1996. ApJ456:902-908

Rose JA 1991. AJ101:937-949

Röser S et al, 1997. in *Hipparcos Venice '97*, eds B Battrick & MAC Perryman (ESA), pp 777-782

Ryan SG, Norris JE 1991. AJ101:1835-1864

Salaris M, Chieffi A, Straniero O 1993. ApJ414:580-600

Sandage A 1958. in *Vatican Conf. Stellar Populations*, ed. D O'Connell, Specola Vaticana 5:41-50

Sandage A, Eggen OJ 1959. MNRAS119:278-291

Sandage A 1970. ApJ162:841-870

Sandage A 1981. ApJ248:161-176

Sandage A 1982. ApJ252:574-581

Sandage A 1986. ARA&A24:421-458

Sandage A 1993a. AJ106:687-701

Sandage A 1993b. AJ106:702-718

Sandage A, Bell RA, Tripicco MJ 1999. ApJ, 522, 250

Sandage A, Tammann GA 1968. ApJ151:531-545

Sandage A, Tammann GA 1998. MNRAS293:L23-L26

Sasselov DD, Beaulieu FP, renault C, Grison P, Ferlet R et al 1996. A&A324:471-482

Schlegel DJ, Finkbeiner DP, Davis M 1998. ApJ500:525-553

Schuster WJ, Nissen PE 1989. A&A221:65-77

Schuster WJ, Parrao L, Contreras Martinez ME 1993. A&AS97:951-983

Schwan H 1991. A&A243:386-400

Seaton MJ, Yan Y, Mihalas D, Pradhan AK 1994. MNRAS266:805-828

Shetrone MD 1997. AJ112:1517-1535

Silbermann N, Smith HA 1995. AJ110:704-728

Simon NR, Clement CM 1993. ApJ410:526-533

Skillen I, Fernley JA, Stobie RS, Jameson RF 1993. MNRAS265:301-315

Smith H 1988. A&A198:365-369

Smith HA 1995. RR Lyrae Stars, Cambridge University Press

Sneden C, Kraft RP, Shetrone MD, Smith GH, Langer GE, Prosser CF 1997. AJ114:1964-1981

Soderblom DR, King JR, Hanson RB, Jones BF, Fischer D, Stauffer J, Pinsonneault, MH 1998. ApJ504:192-199

Stanek KZ, Garnavich PM 1998. ApJ503:L131-L134

Storm JS, Carney BW, Latham DW 1994. A&A290:443-457

Straniero O 1988. A&AS76:157-184

Straniero O, Chieffi A 1991. ApJS76:525-616

Straniero O, Chieffi A, Limongi M 1997. ApJ490:425-436

Strugnell P, Reid N, Murray CA 1986. MNRAS220:413-427

Sturch CR 1966. ApJ143:774-808

Sweigart AV, Gross PG 1976. ApJS32:367-398

Sweigart AV 1997. ApJ474:L23-L26

Torres G, Stefanik RP, Latham DW 1997. ApJ485:167-181

Tsujimoto T, Miyamoto M, Yoshii Y 1998. ApJ492:L79-L82

Trumpler RJ, Weaver HF 1953. Statistical Astronomy, Berkeley University Press

Udalski A, Szymański M, Kubiak M, Pietrzyński G, Woźniak P, Żebruń LK 1998. Acta Astr 48:1-17 van Albada TS, Baker N 1971. ApJ169:311-326

van Albada TS, Baker N 1973. ApJ185:477-498

van Leeuwen F 1997 Sp. Sci. Rev. 81, 201-409

van Leeuwen F, Feast MW, Whitelock PA, Yudin B 1997. MNRAS287:955-960

van Leeuwen, F, Hansen Ruiz, CS 1997. in *Hipparcos Venice '97*, ed B Battrick (ESA), 689-692

van Leeuwen F 1999 A&A341:L71-L74

Vandenberg DA, Bolte M, Stetson PB 1990. AJ100:445-468

Walker AR 1992. ApJ390:L81-L84

Walker AR 1994. AJ108:555-584

Walker AR 1998. in Post-Hipparcos Cosmic Candles, eds. F. Caputo & A. Heck, Kluwer Acad. Publ, Dordrecht

Walker AR, Mack P 1988. AJ96:872-876

Walker AR, Terndrup DW 1991. ApJ378:119-126

Wan L, Mao Y-Q, Ji D 1980. Ann Shanghai Obs Acad Sinica 2:1

Wesselink AJ 1946. Bull Astr Inst Netherlands 10:91-98

Wyse RFG, Gilmore G 1995. AJ110:2771-2787

Zinn R, West MJ 1984. ApJS55:45-66

This preprint was prepared with the AAS LaTeX macros v4.0.

Table 1: Globular cluster abundances

Cluster	[Fe/H]$_C$	[Fe/H]$_{ZW}$	[Fe/H]$_{LT}$	[O/Fe]$_{LT}$	[Fe/H]$_{CG}$
M71	-0.7	-0.58	-0.79	0.2	-0.70
M5	-1.4	-1.40	-1.17	0.35/-0.25	-1.11
M3	-1.8	-1.66	-1.47	0.3/-0.2	-1.34
M13	-1.6	-1.65	-1.49	0.3/-0.15/-0.6	-1.39
M10		-1.60	-1.52	0.3	-1.41
M92	-2.35	-2.24	-2.25	0.3/-0.05	-2.16
M15	-2.20	-2.17	-2.40	0.2	-2.12

Table 2: Main-sequence fitting distance determinations

Cluster	E_{B-V}(IR) V_{TO}	$[Fe/H]_{CG}$	Harris E_{B-V}	Rees/WD E_{B-V}	DCM E_{B-V}	R97 E_{B-V}	G97 E_{B-V}	CDKK[1] E_{B-V}	R98
47 Tuc	0.03	-0.70	13.17				13.47		13.56
	17.65		0.05				0.055		0.04
M71	0.34	-0.70	12.92						13.19
	18.00		0.25						0.28
NGC 288	0.015	-1.07	14.55				14.85		15.00
	19.02		0.03				0.03		0.01
M5	0.045	-1.11	14.32	14.4±.4		14.45	14.51	14.42	14.52
	18.48		0.03			0.03	0.035	0.03	0.02
NGC 362	0.035	-1.15	14.60				14.88		14.79[2]
	18.80		0.05				0.055		0.04
M4[3]	0.495	-1.19	11.41	11.2±.2					
	16.90		0.36						
M3	0.015	-1.34	15.01	14.9±.6					15.10[4]
	19.14		0.01						0.01
M13	0.02	-1.39	14.22	14.06±.23		14.48	14.41		14.45
	18.50		0.02			0.02	0.02	0.02	0.02
NGC 6752	0.06	-1.41	12.96	13.05^{WD}		13.17	13.24	13.20	13.16
	17.30		0.04	0.04		0.02	0.035	0.04	0.04
NGC 6397	0.18	-1.82	11.75						12.24
	16.60		0.18						0.18
M30	0.06	-1.91	14.46		14.80	14.95	14.84		14.85[5]
	18.60		0.03		0.04	0.05	0.04		0.04
M68[6]	0.07	-1.99	15.01		15.10	15.24	15.15		15.15[5]
	19.05		0.04		0.06	0.05	0.04		0.06
M15	0.10	-2.12	15.03			15.38			15.23[5]
	19.40		0.09			0.09			0.09
M92[7]	0.02	-2.16	14.54	14.76±.3	14.80	14.93	14.74	14.76	14.78[5]
	18.60		0.02		0.02	0.02	0.02	0.02	0.02

Globular cluster distance moduli and reddening:
Column 2 lists E_{B-V} deduced from 100 μm maps (Schlegel et al (1998)) and the apparent magnitude (uncorrected for reddening) at the turnoff;
column 3 gives the abundance on the Carretta & Gratton (1997 -CG97) scale.
Succeeding columns list derived distance moduli and adopted reddenings from individual investigations: column 4, from the pre-Hipparcos compilation by Harris (1996); column 5, astrometric distances from Rees (1996) and WD-fitting distance for NGC 6752 (Renzini et al, 1996); column 6, from D'Antona, Caloi & Mazzitelli (1997 - DCM); column 7, Reid (1997 - R97); column 7, Gratton et al (1997b - G97); column 9, Chaboyer et al (1998 - CDKK); and column 10, data from Reid (1998) and Reid & Gizis (1998 - RG98).
The G97, CDKK, R98 and RG98 analyses are tied to the CG97 abundance scale and use subdwarf metallicities from GCC and AFG. The remaining studies adopt the Zinn & West cluster abundances and, in most cases, CLLA's subdwarf metallicities.
Notes:
[1] Main-sequence fitting distance estimates only
[2] Relative distance modulus (Vandenberg et al, 1990) with respect to M5
[3] R=3.8 is assumed for M4
[4] Based on matching the turnoff region against M13 (Reid & Gizis, 1998)
[5] Relative distance moduli with respect to NGC 6397 (Reid & Gizis, 1998)
[6] MS-fitting results adjusted to match photometry from Walker (1994)
[7] Pont et al (1998) derive $(m-M)_0$=14.67 for E_{B-V}=0.02 for M92.

Table 3: RR Lyrae statistical parallax analyses

Source	$\langle M_V \rangle$	n_*	$\langle [Fe/H] \rangle$	U	V	W	σ_U	σ_V	σ_W
Hawley et al[a]	0.79±0.21	65	-0.7	5	-120	-14	128	120	78
	0.73±0.18	65	1.5	-21	-184	-4	166	114	91
Strugnell et al[b]	0.90±0.21	64	-0.68	4	-110	-17	124	109	70
	0.85±0.19	75	-1.43	-2	-185	-3	161	108	94
Layden et al	0.94±0.30[c]	51	-0.76	6	-45	-16	52	48	29
	0.71±0.12[d]	162	-1.61	9	-210	-12	168	102	97
Fernley et al	0.77±0.15	84	-1.66						
	0.69±0.21	60	-0.85						
Tsujimoto et al	0.69±0.10	99	-1.58	-12	-200	1	160	104	86
Gould & Popowski	0.77±0.13[e]	147	-1.60	6	15	1	171	99	90

[a] Reddenings based on Sturch's (1966) method

[b] Reddenings based on Burstein & Heiles (1982) HI maps

[c] Disk-3 sample

[d] Halo-3 sample

[e] Subset of Halo-3 sample

Fig. 1.— Formal uncertainties in Hipparcos astrometry as a function of apparent magnitude - the sample consists of stars drawn from the Lowell Observatory proper motion survey.

Fig. 2.— Hipparcos-based (M_V, (B-V)) data for nominally-single nearby stars from Wyse & Gilmore's analysis of the local abundance distribution. The dashed lines are 1- and 5-Gyr isochrones from Bertelli et al (1994) for [Fe/H]=0.0 and -0.4 dex; the solid line is the mean relation described by local stars (Reid & Murray, 1992).

Fig. 3.— (M_V, (B-V)) data for single subdwarfs with abundance determinations by Gratton et al (1997) or Axer et al (1994) compared against 12-Gyr isochrones predicted by D'Antona et al (1997) for [Fe/H]=-0.7, -1.0, -1.5 and -2.0.

Fig. 4.— a: the predicted relation between M_V(TO) and [Fe/H] for 12, 14 and 16 Gyrs given by Bergbusch & Vandenberg (solid lines), Straniero & Chieffi (dashed lines) and D'Antona, Caloi & Mazzitelli (dotted); b: M_V(TO) deduced for clusters in Table 2 (except the highly-reddened M4) compared to the DCM predictions for ages of 10, 12, 14 and 16 Gyrs. The models have [α/Fe]=0 and are therefore offset by -0.2 dex.

Fig. 5.— (M_V, T_{eff}) and (M_V, (B-V)) isochrones predicted for 12-Gyr old metal-poor systems by Bergbusch & Vandenberg (BV92) and D'Antona et al (DCM). The former models adopt [O/Fe]=+0.4 while the latter have scaled-solar abundance ratios. To allow for this we compare the BV92 [Fe/H]=-2.26 model against the [Fe/H]=-2.03 DCM isochrone.

Fig. 6.— A summary of the various RR Lyrae (M_V, [Fe/H]) relations. The five solid points mark $\langle M_V \rangle$ for M5, M13, M15, M68 and M92 variables, using the distance moduli given in the final column of Table 2. The dotted horizontal lines mark the 1σ limits deduced in the Layden et al statistical-parallax analysis, while the upper histogram plots the abundance distribution of field RR Lyraes.

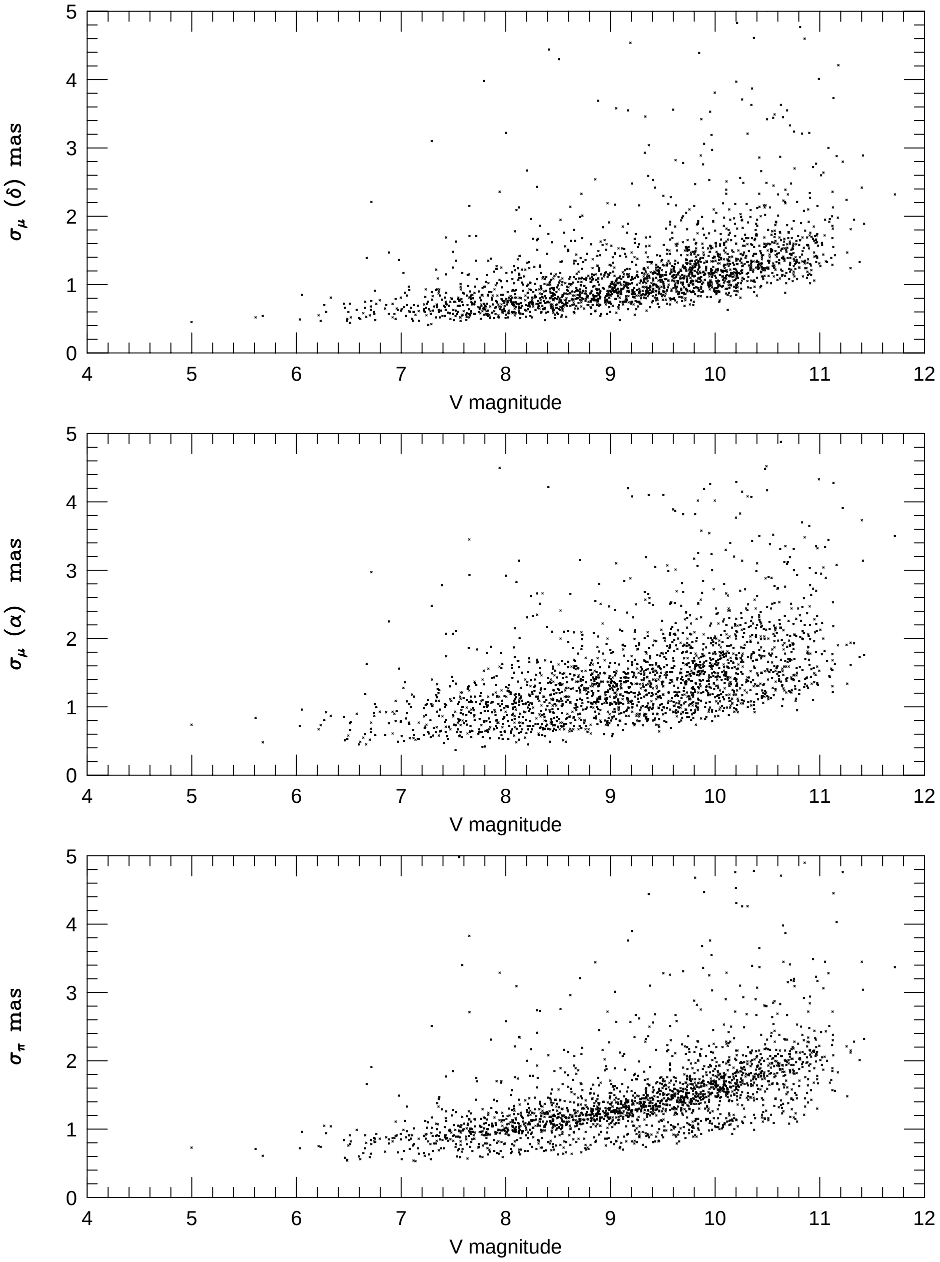

5
4
3
2
1
0
σ_μ (δ) mas
4
5
6
7
8
9
10
11
12
V magnitude
5
4
3
2
1
0
σ_μ (α) mas
4
5
6
7
8
9
10
11
12
V magnitude
5
4
3
2
1
0
σ_π mas
4
5
6
7
8
9
10
11
12
V magnitude

Fig. 1.—

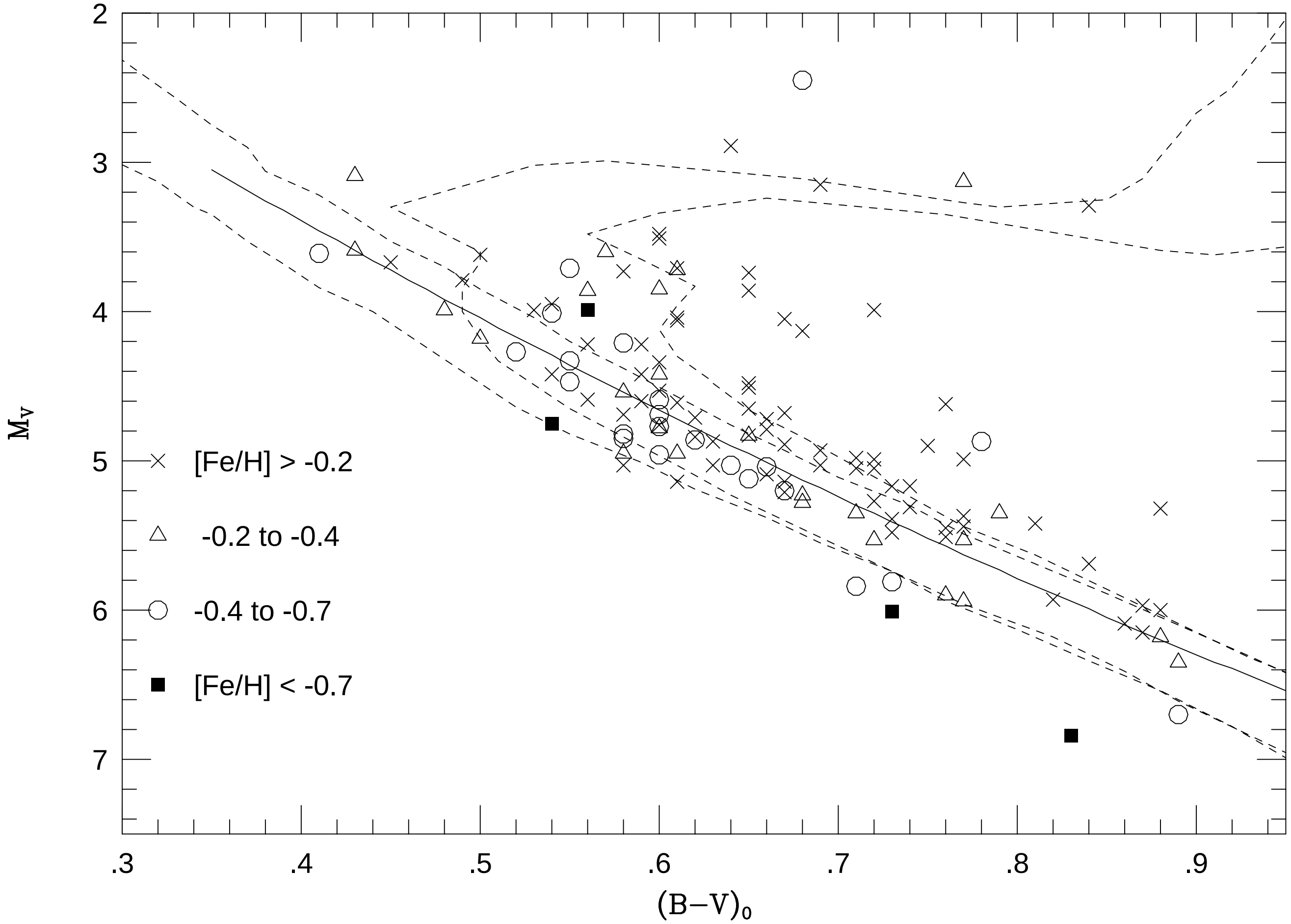

Fig. 2.—

Fig. 3.—

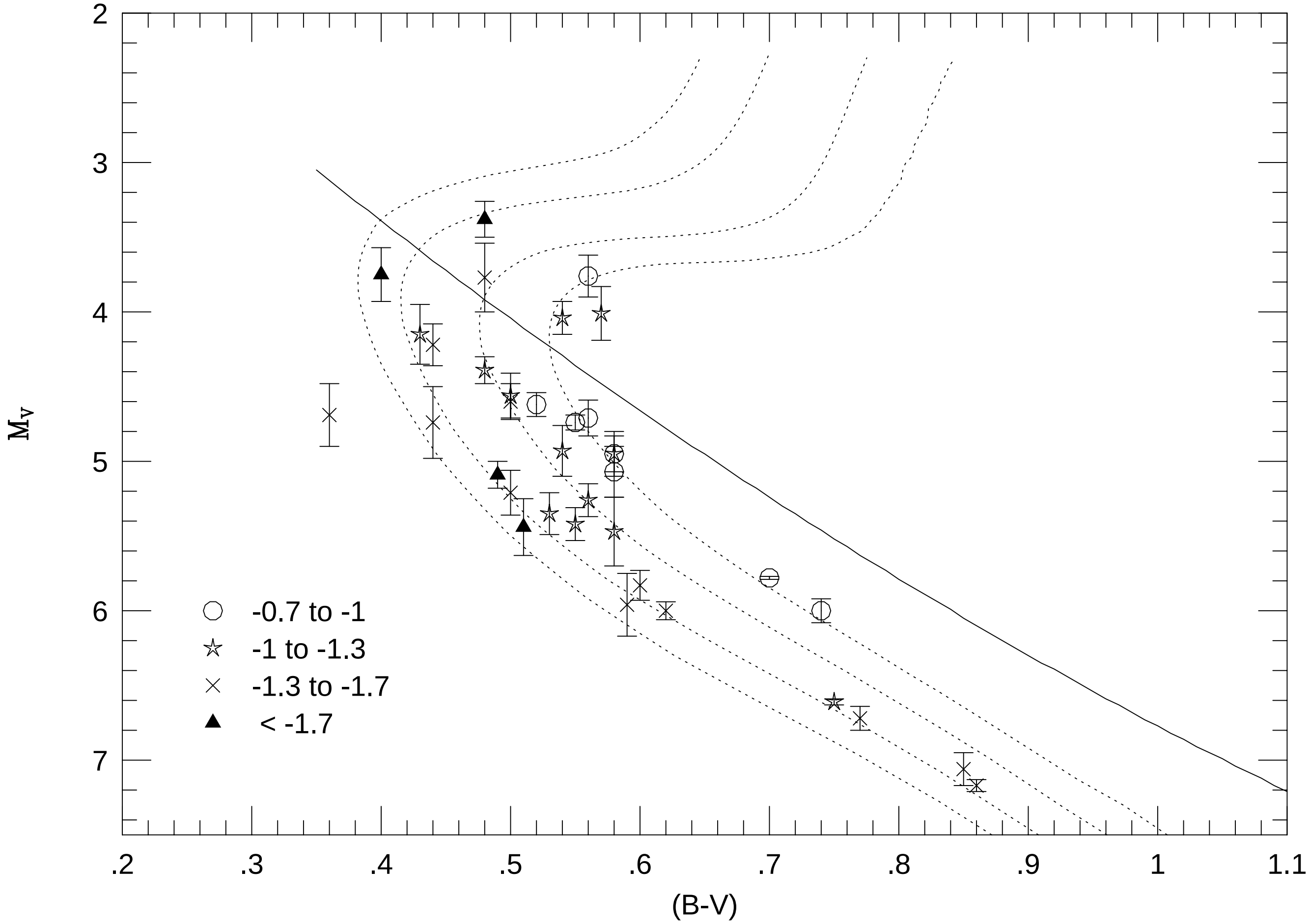

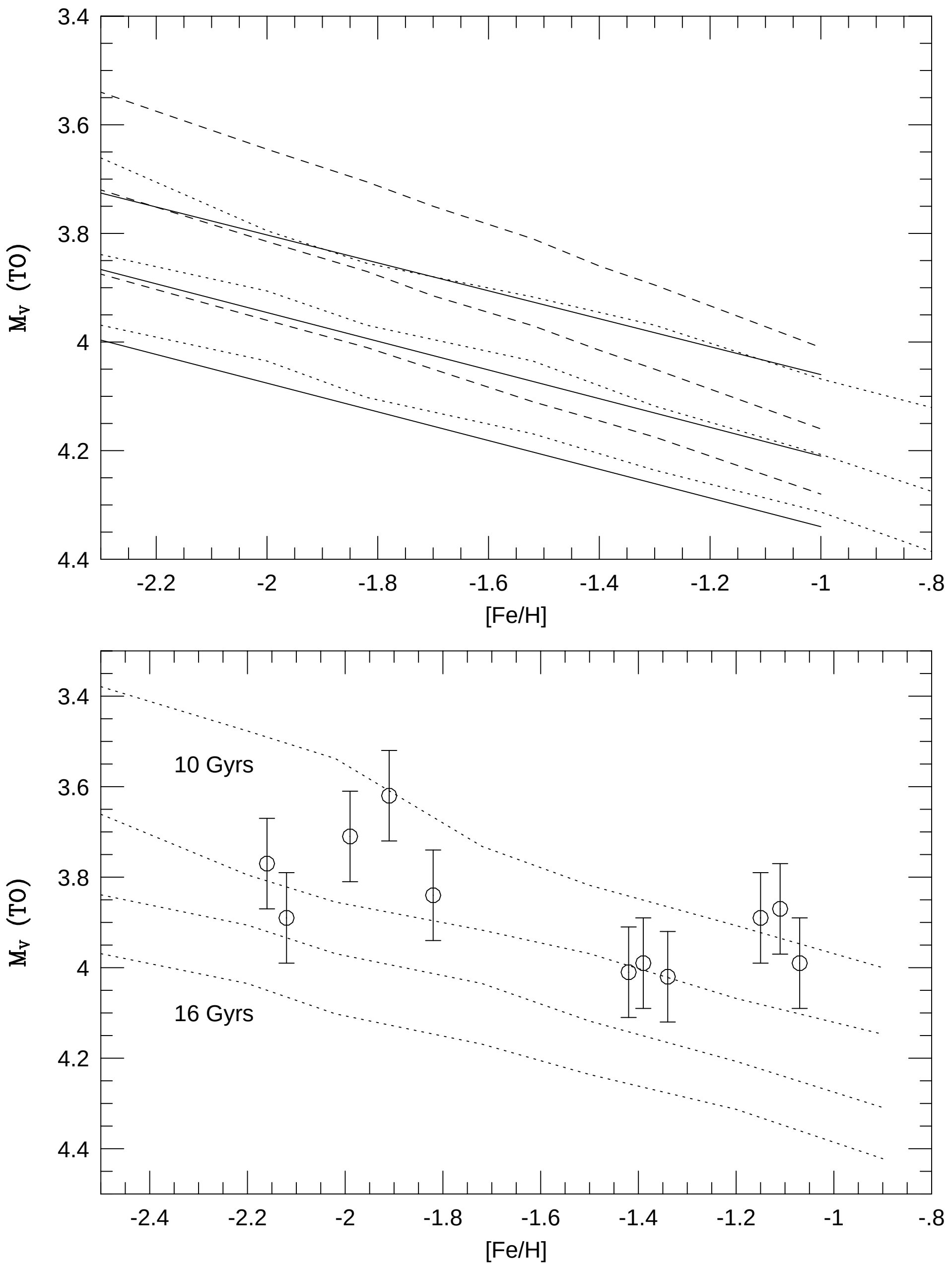

Fig. 4.—

Fig. 5.—

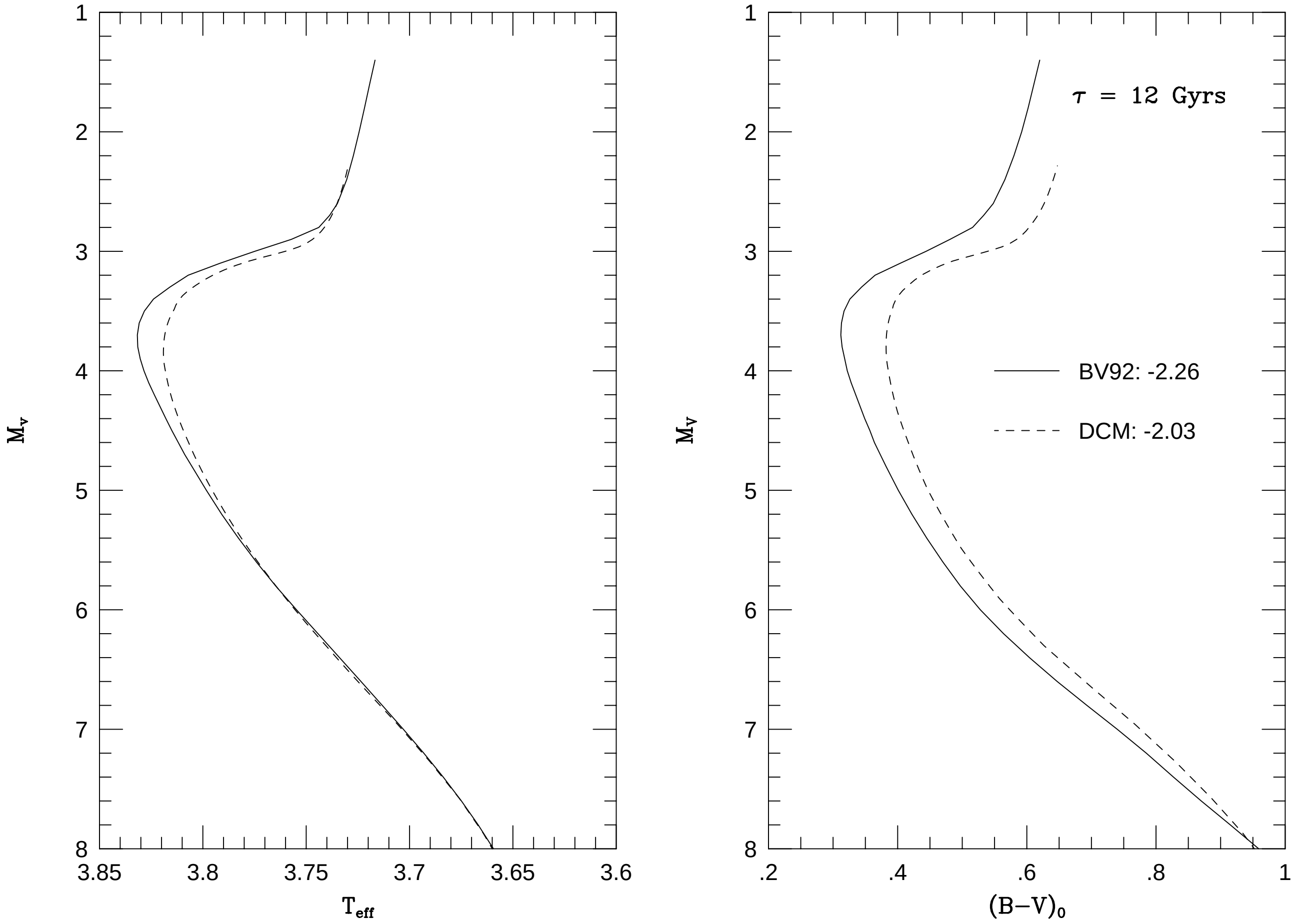

τ = 12 Gyrs
BV92: -2.26
DCM: -2.03
M_V
T_{eff}
$(B-V)_0$
1
2
3
4
5
6
7
8
3.85
3.8
3.75
3.7
3.65
3.6
.2
.4
.6
.8
1

Fig. 6.—

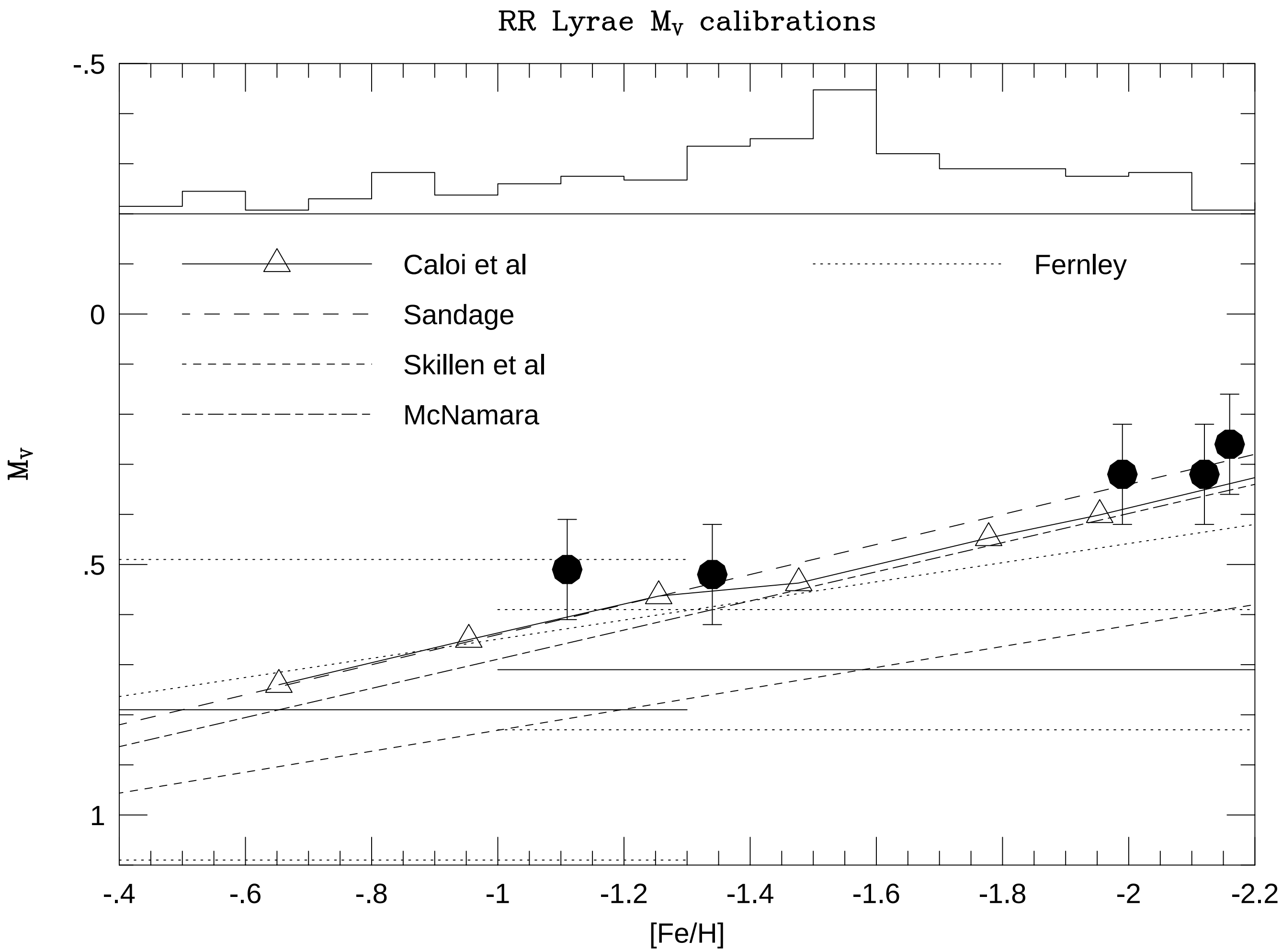
RR Lyrae M_V calibrations
M_V
[Fe/H]
Caloi et al
Sandage
Skillen et al
McNamara
Fernley
-.5
0
.5
1
-.4
-.6
-.8
-1
-1.2
-1.4
-1.6
-1.8
-2
-2.2